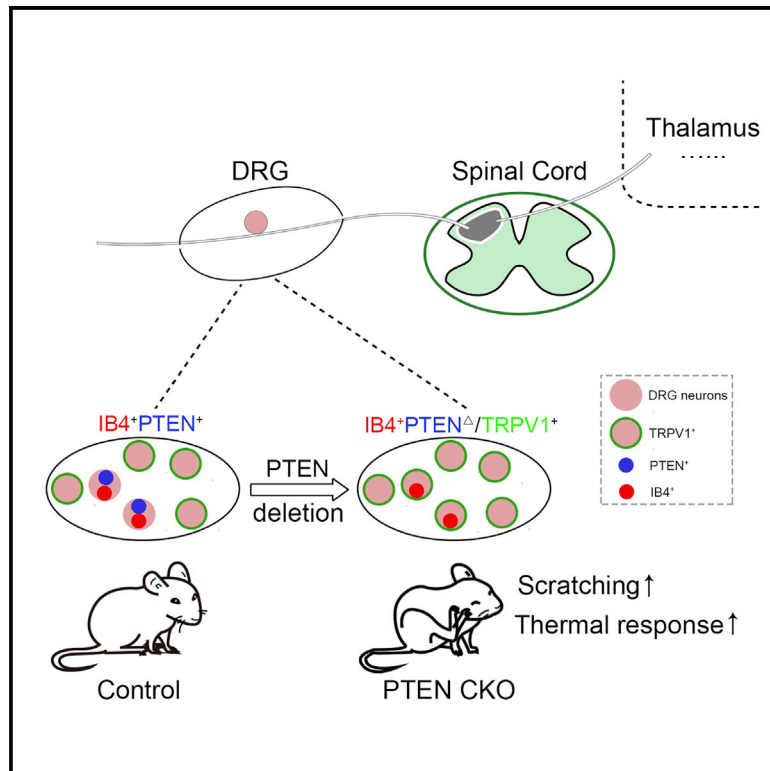# The role of PTEN in primary sensory neurons in processing itch and thermal information in mice

Graphical abstract

Authors

Ling Hu, Guan-Yu Jiang,
Ying-Ping Wang, ..., Yong Li,
Qing-Xiu Wang, Yu-Qiang Ding

Correspondence

qxw1123@126.com (Q.-X.W.),
dingyuqiang@vip.163.com (Y.-Q.D.)

In brief

Hu et al. report that PTEN, a tumor-suppressor gene, is involved in processing itch and thermal information in adult mice. They reveal that PTEN also suppresses expression of itch-related genes in primary sensory neurons and when defective leads to elevated itch and thermal sensation at the spinal level.

Highlights

- PTEN is mainly expressed in $IB4^+$ non-peptidergic dorsal root ganglion (DRG) neurons

- Adult deletion of *PTEN* in DRG leads to augmented itch and enhanced thermal nociception

- $TRPV1^+$ neurons are significantly increased in the DRG of *PTEN* CKO mice

- Ectopic TRPV1 expression in DRG neurons causes itch and thermal responses in *PTEN* CKO

CellPress

Article

The role of PTEN in primary sensory neurons in processing itch and thermal information in mice

Ling Hu,[1,2,3,8] Guan-Yu Jiang,[3,8] Ying-Ping Wang,[4,8] Zhi-Bin Hu,[2] Bing-Yao Zhou,[2] Lei Zhang,[3] Ning-Ning Song,[1,2] Ying Huang,[1] Guo-Dong Chai,[5] Jia-Yin Chen,[1,3] Bing Lang,[6] Lin Xu,[7] Jun-Ling Liu,[4] Yong Li,[4] Qing-Xiu Wang,[5,*] and Yu-Qiang Ding[1,2,3,9,*]

[1]Department of Laboratory Animal Science, Fudan University, Shanghai 200032, China
[2]State Key Laboratory of Medical Neurobiology and MOE Frontiers Center for Brain Science, Institutes of Brain Science, Fudan University, Shanghai 200032, China
[3]Key Laboratory of Arrhythmias, Ministry of Education, East Hospital, and Department of Anatomy and Neurobiology, Tongji University School of Medicine, Shanghai 200092, China
[4]Department of Biochemistry and Molecular Cell Biology, Shanghai Key Laboratory for Tumor Microenvironment and Inflammation, Institute of Medical Sciences, Shanghai JiaoTong University School of Medicine, Shanghai 200025, China
[5]Department of Anesthesiology, East Hospital, Tongji University School of Medicine, Shanghai 200120, China
[6]Department of Psychiatry, The Second Xiangya Hospital, Central South University, Changsha, Hunan 410011, China
[7]Laboratory of Learning and Memory, Kunming Institute of Zoology, Chinese Academy of Sciences, Kunming 650223, China
[8]These authors contributed equally
[9]Lead contact
*Correspondence: qxw1123@126.com (Q.-X.W.), dingyuqiang@vip.163.com (Y.-Q.D.)
https://doi.org/10.1016/j.celrep.2022.110724

SUMMARY

PTEN is known as a tumor suppressor and plays essential roles in brain development. Here, we report that PTEN in primary sensory neurons is involved in processing itch and thermal information in adult mice. Deletion of *PTEN* in the dorsal root ganglia (DRG) is achieved in adult *Drg11*-Cre[ER]: *PTEN*[flox/flox] (*PTEN* CKO) mice with oral administration of tamoxifen, and CKO mice develop pathological itch and elevated itch responses on exposure to various pruritogens. *PTEN* deletion leads to ectopic expression of TRPV1 and MrgprA3 in IB4^{+} non-peptidergic DRG neurons, and the TRPV1 is responsive to capsaicin. Importantly, the elevated itch responses are no longer present in *Drg11*-Cre[ER]: *PTEN*[flox/flox]: *TRPV1*[flox/flox] (*PTEN*: *TRPV1* dCKO) mice. In addition, thermal stimulation is enhanced in *PTEN* CKO mice but blunted in dCKO mice. PTEN-involved regulation of itch-related gene expression in DRG neurons provides insights for understanding molecular mechanism of itch and thermal sensation at the spinal level.

INTRODUCTION

Itch sensation is generated in the skin and mucus membrane by the peripheral terminals of primary sensory neurons located in the dorsal root ganglia (DRG) and trigeminal ganglia (Bautista et al., 2014; Braz et al., 2014; Han and Dong, 2014; Ross, 2011). Acute itch is produced by activation of the terminals by various pruritogens, while chronic itch is often caused by central and/or peripheral sensitization in the itch-related somatosensory pathway and often occurs in chronic dermatosis and diseases in other systems, such as chronic liver diseases (Akiyama and Carstens, 2013). Recently, substantial progress has been made in dissecting the mechanism underlying itch sensation.

At the primary sensory level, itch-inducing molecules activate multiple membrane-bound receptors in the peripheral terminals, such as histamine receptors (Inagaki et al., 1999; Rossbach et al., 2009), proteinase activated receptors (PAR) 2 and 4 (Reddy et al., 2008; Steinhoff et al., 2000, 2003), endothelin-1 receptor subtype A (McQueen et al., 2007), and Toll-like receptor 7 (Liu et al., 2010a). Recently, several Mas-related G-protein-

coupled receptor (Mrgpr) members expressed by primary sensory neurons have been reported to be required for processing itch-related sensory input. For example, MrgprA3, MrgprD, and MrgprC11 expressed in small-diameter DRG neurons are responsible for itch responses induced by chloroquine, β-alanine, and bovine adrenal medulla peptide, respectively (Dong et al., 2001; Liu et al., 2009, 2011, 2012). Furthermore, transient receptor potential (TRP) channel subfamily V member 1 (TRPV1) is required for the histamine-induced itch response (Davidson and Giesler, 2010; Imamachi et al., 2009; Shim et al., 2007), while another TRP channel, TRPA1, is required for histamine-independent itch transmission (Wilson et al., 2011). Because of the colocalization of TRPV1 with multiple itch-related receptors in DRG neurons, TRPV1^{+} neurons are also required for 5-HT-, endothelin-1-, imiquimod-, and chloroquine-induced itch responses (Inagaki et al., 1999; Liu et al., 2010b; Roberson et al., 2013).

At the spinal level, B-type natriuretic polypeptide (NPPB)-containing primary pruriceptors release NPPB and glutamate to activate secondary pruriceptors expressing both the NPPB receptor
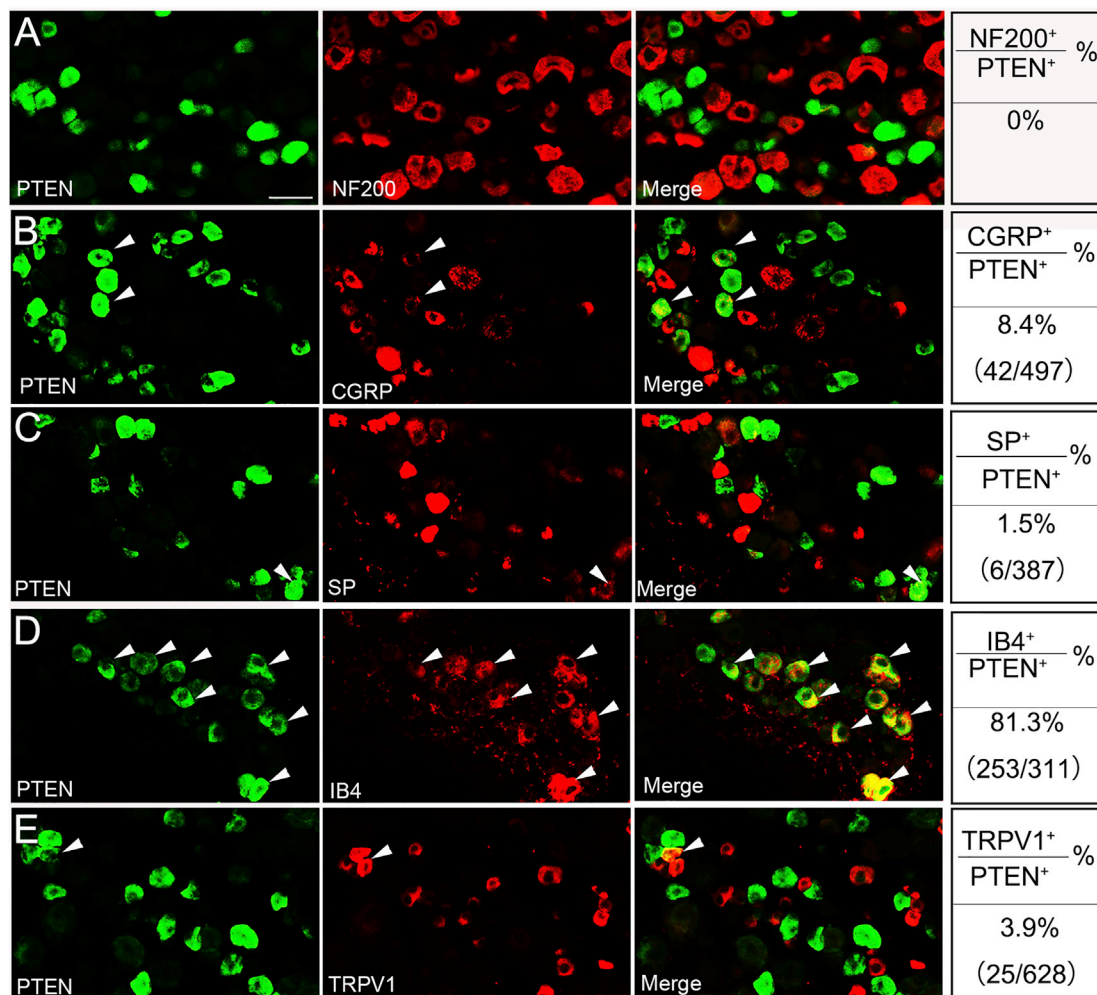
Figure 1. PTEN is mainly expressed in the IB4+ population in the DRG
(A–E) Double staining of PTEN with NF200 (A), CGRP (B), SP (C), IB4 (D), and TRPV1 (E). n = 3 for each double staining. Triangles indicate double-labeled neurons. Scale bar, 50 μm in (A) and applies in (B)–(E).

and gastrin-releasing peptide (GRP) in the spinal dorsal horn (Bautista et al., 2014; Koga et al., 2011; Mishra and Hoon, 2013; Sun et al., 2017), and itch-related information is then transmitted to spinal tertiary pruriceptors expressing the GRP receptor (GRPR). Finally, this information is transmitted to supraspinal regions via a relay of spinal ascending neurons (Bautista et al., 2014; Davidson et al., 2009; Jiang et al., 2015; Mu et al., 2017; Sun et al., 2009; Sun and Chen, 2007). In contrast, glutamate released from activated TRPV1-expressing nociceptors activates Bhlhb5-expressing inhibitory interneurons, which release dynorphin (DYN) and somatostatin (SST) to inhibit itch transmission (Bautista et al., 2014; Huang et al., 2018; Kardon et al., 2014; Lagerström et al., 2010; Liu et al., 2010b; Patel and Dong, 2010; Ross et al., 2010).

PTEN is a tumor-suppressor gene encoding a protein with phosphatase activity that functions as a brake of the PI3K-Akt signaling pathway by hindering Akt activation (Di Cristofano et al., 1998; Li et al., 1997; Steck et al., 1997; Suzuki et al.,

1998; Worby and Dixon, 2014). PTEN mutations are present in autistic individuals with macrocephaly (Butler et al., 2005; Goffin et al., 2001; Zori et al., 1998), and these mutations have been shown to play biological roles in brain development, including the regulation of neural stem cell proliferation, neuronal arborization, and soma size (Diaz-Ruiz et al., 2009; Groszer et al., 2001; Kwon et al., 2006). In the adult nervous system, the inactivation of PTEN in retinal ganglion cells and DRG neurons promotes axonal regeneration of the optic nerve and sciatic nerve, respectively, and lowering PTEN activity shows a beneficial effect on axonal regeneration of the injured pyramidal tract (Christie et al., 2010; Gregorian et al., 2009; Kwon et al., 2006; Li et al., 2003; Park et al., 2008). PTEN expression in the pyramidal neurons of the prefrontal cortex and serotonergic neurons of the raphe nucleus plays a key role in regulating depression status via regulating the morphological complexity of those neurons (Chen et al., 2021; Wang et al., 2021). In this study, we explored the role of PTEN in processing itch and thermal information by
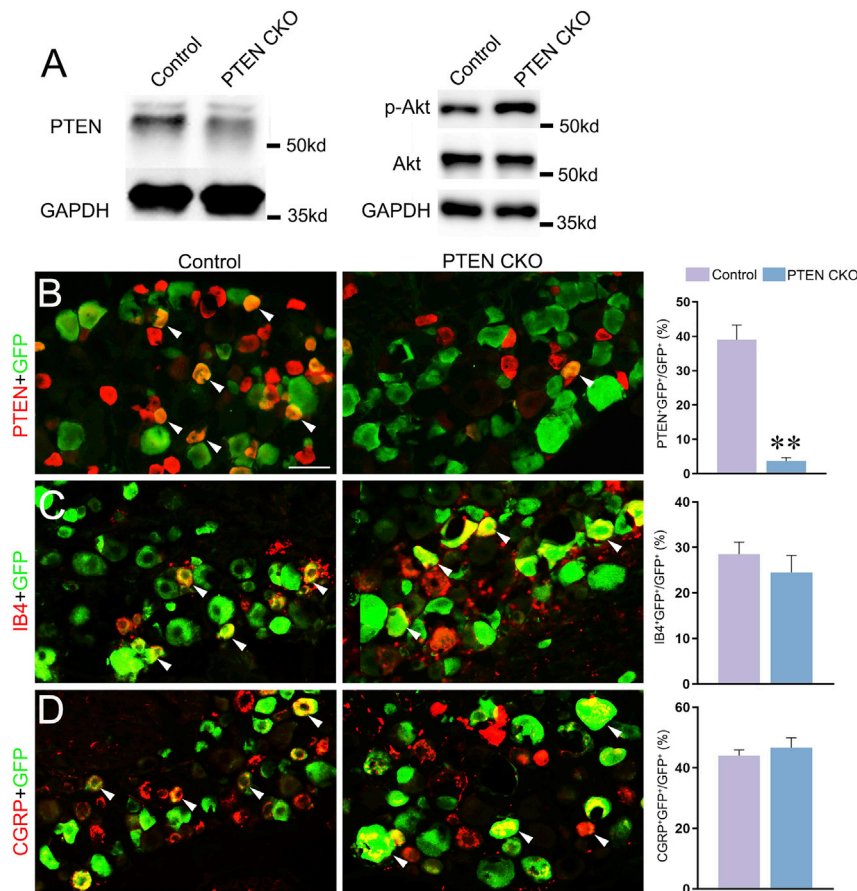
selective deletion PTEN in a population of DRG neurons in adult mice and found that the deletion leads to pathological itch, and the elevations of pruritogen-induced itch responses and thermal sensitivity, thus revealing a new role for PTEN in regulating itch and thermal sensation at the spinal level.

RESULTS

PTEN is primarily expressed in the IB4^{+} population in the DRG

To investigate the cellular expression profile of PTEN, we performed double immunostaining of PTEN with different markers of DRG neurons. First, no colocalization of PTEN and neurofilament-200 (NF200) was detected in DRG neurons of control mice (Figure 1A), showing that PTEN is not expressed in large NF200^{+} DRG neurons. Next, we performed double immunostaining of PTEN with calcitonin gene-related peptide (CGRP), which is primarily expressed in small and medium-sized DRG neurons (Lawson and Waddell, 1991), and found that approximately 8.4% of PTEN^{+} neurons expressed CGRP (Figure 1B). Similarly, a few neurons (∼1.5%) positive for substance P (SP), a marker for small peptidergic DRG neurons, were also labeled with PTEN immunoreactivity (Figure 1C). We performed double staining of PTEN with isolectin B4 (IB4), a marker for small non-peptidergic DRG neurons (Silverman and Kruger, 1988). Consistent

with previous data (Christie et al., 2010), the majority (∼81.3%) of PTEN^{+} neurons were also labeled with IB4, which corresponded to ∼85.0% of IB4^{+} neurons (Figure 1D). We noticed that only a small fraction (∼3.9%) of PTEN^{+} neurons expressed TRPV1 (Figure 1E). Thus, PTEN is primarily expressed in small non-peptidergic DRG neurons in adult mice.

PTEN deletion in DRG neurons

Selective deletion of *PTEN* in DRG neurons was achieved by crossing *Drg11*-Cre[ER] mice (Hu et al., 2012) with *PTEN*[flox/flox] mice (Lesche et al., 2002) to obtain *Drg11*-Cre[ER]: *PTEN*[flox/flox] (*PTEN* CKO) mice. Littermates with other genotypes (i.e., *PTEN*[+/flox] and *PTEN*[flox/flox]) were used as controls, and heterozygous PTEN CKO mice (*Drg11*-Cre[ER]: *PTEN*[flox/+]) were not analyzed in this study. The CKO and control mice received oral administration of tamoxifen at 2 months of age and were subjected to various examinations 3 weeks later.

Western blot analysis showed that the total PTEN protein level was dramatically decreased in the DRG neurons of the CKO mice relative to the control, whereas the level of serine 473 phosphorylated Akt (p-Akt), which is negatively regulated by PTEN (Dibble and Cantley, 2015), was significantly increased (Figure 2A). To show *PTEN* deletion at the cellular level, *Drg11*-Cre[ER]: *Rosa*26-stop-YFP (control) and *PTEN* CKO: *Rosa*26-stop-YFP mice were generated, and Cre-expressing neurons were visualized by GFP immunostaining. PTEN was present in ∼39% of GFP[+] (i.e., Cre^{+}) neurons in control mice, and most PTEN[+]/GFP^{+} neurons were small in size (Figure 2B), consistent with the predominant distribution of PTEN in IB4^{+} neurons. In contrast, a very small fraction of (∼3%) PTEN[+]/GFP^{+} neurons was detected in *PTEN* CKO: *Rosa*26-stop-YFP mice (Figure 2B), showing the successful deletion of *PTEN* in *PTEN* CKO mice. The percentages of IB4^{+}/GFP^{+} neurons and CGRP[+]/GFP[+] in the total population of GFP^{+} cells were not obviously changed (Figures 2C and 2D). Thus, *PTEN* was successfully deleted in a population of DRG neurons of *PTEN* CKO mice after tamoxifen treatment in adulthood.
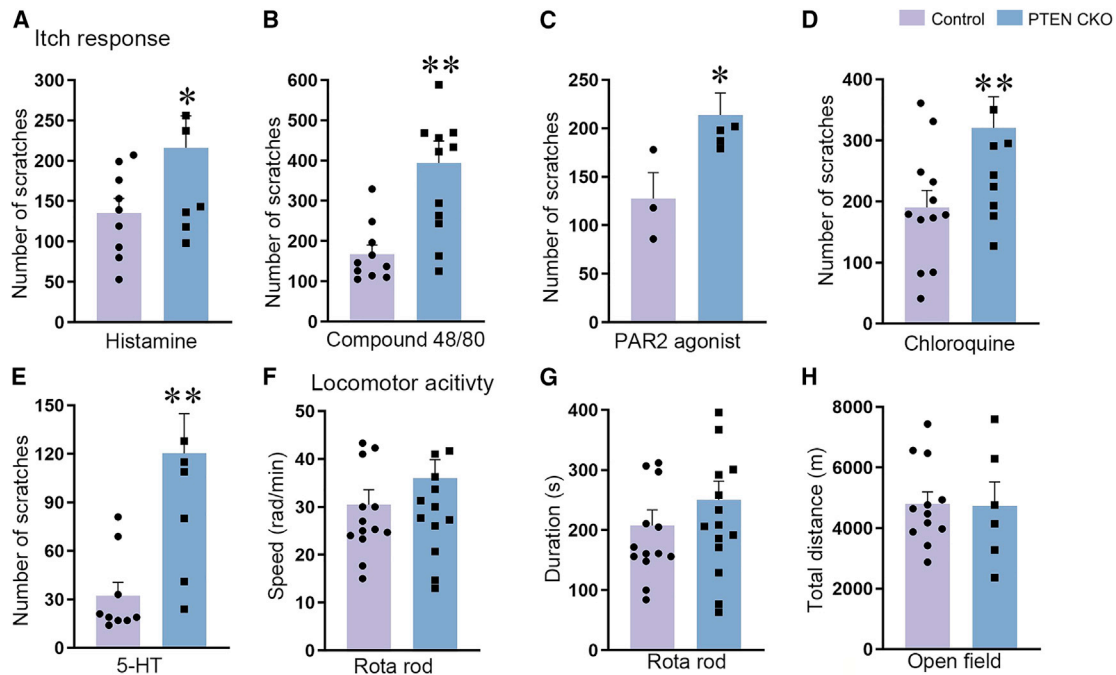
Figure 3. Elevated pruritogen-induced itch responses in *PTEN* CKO mice

(A–E) Intradermal injection of histamine (n = 10 for control and n = 9 for CKO mice, A), compound 48/80 (n = 10 for control and n = 12 for CKO mice, B), PAR2 agonist (n = 3 for control and n = 5 for CKO mice, C), chloroquine (n = 13 for control and n = 14 for CKO mice, D), and 5-HT (n = 9 for control and n = 10 for CKO mice, E) induced significant elevation of scratches in *PTEN* CKO mice compared with that in controls. Bars represent ±SEM. Student's t test *p < 0.05, **p < 0.01.

(F and G) The maximal speed of the rod and duration spent on the rod were not changed (n = 14 for control and n = 16 for CKO mice) in the *PTEN* CKO mice relative to that in the controls. Bars represent ±SEM.

(H) The total distance traveled in the open field test was comparable between controls and *PTEN* CKO mice (n = 12 for control and n = 6 for CKO mice). Bars represent ±SEM.

Spontaneous itch behaviors in *PTEN* CKO mice

In *PTEN* CKO mice, visible skin lesions at the craniofacial region, legs, and tail existed 2 months after the last tamoxifen administration with an incidence of ∼27% (3 of 11). Skin lesion incidence increased over time. After 3 additional months, more mice had skin lesions, with the incidence reaching ∼42% (5 of 12). Eventually skin lesions were observed in ∼83% (5 of 6) of the mice 7 months after tamoxifen administration. We assessed the intensity of spontaneous scratching to reflect the time course of spontaneous itch development. This spontaneous scratching increased over time, as shown by the data that "itchy" mice scratched 57.7 ± 22.1 and 207.6 ± 23.3 times per 30 min 2 and 4 months after the last tamoxifen administration, respectively. Notably, their littermates showed much fewer scratches at these two time points (13.1 ± 3.4 and 15.2 ± 6.2, respectively). These results indicate that *PTEN* deletion in primary sensory neurons results in spontaneous itch.

Elevated pruritogen-induced itch responses in *PTEN* CKO mice

We next assessed itch responses induced by multiple pruritogens in *PTEN* CKO mice. This analysis was performed 3 weeks after tamoxifen administration, at which time the CKO mice had not yet developed excessive spontaneous scratching or skin lesions. Histamine is one of the best evaluated itch mediators and acts on a subset of mechanically insensitive C-fibers

that express HR1 and HR4 as well as TRPV1 for itch sensation (Bautista et al., 2014). When injected into the dorsal nape skin, histamine induced a 2-fold increase in scratching responses in *PTEN* CKO mice compared with that in their littermate controls (Figure 3A), indicating an augmented itch response to histamine in *PTEN* CKO mice. In addition, compound 48/80, which activates the histamine-dependent itch pathway (Liu et al., 2010a), also induced more intense scratching responses in *PTEN* CKO mice than in controls (Figure 3B). Thus, the sensation of histamine-dependent itch is augmented in *PTEN* CKO mice.

Protease-activated receptor 2 (PAR2) activates a histamine-independent itch pathway (Liu et al., 2010a). Intradermal injection of PAR2 agonists into the dorsal nape induced a 2-fold increase in scratching bouts in CKO mice compared with that in controls (Figure 3C). Chloroquine is another well-known non-histaminergic itch-inducing reagent (Han et al., 2013) and induced a more intense scratching response in *PTEN* CKO mice (Figure 3D). 5-HT also induced an itch response (Kim et al., 2008; Yamaguchi et al., 1999). A low dose of 5-HT elicited a moderate itch response in control mice, whereas the itch response was remarkably elevated 4-fold in *PTEN* CKO mice (Figure 3E). Overall, both histamine-dependent and histamine-independent acute itch responses are augmented in *PTEN* CKO mice.

Finally, locomotion activity was assessed by the rotarod and open field tests. No differences in the maximum speed
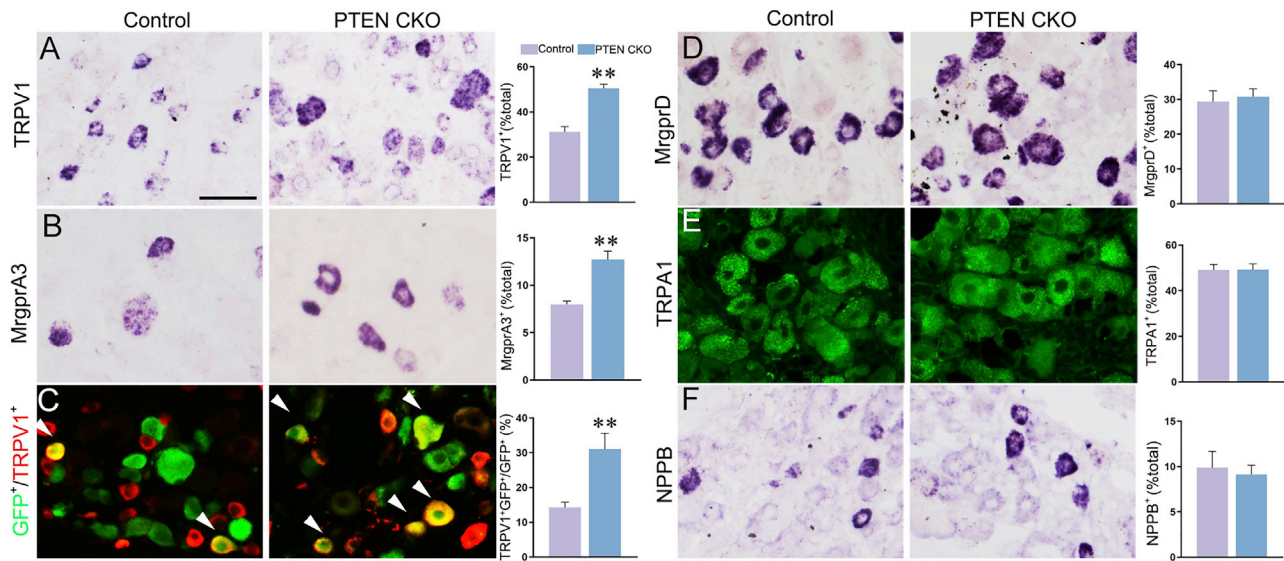
Figure 4. Upregulation of the expression of itch-related genes in the DRG neurons of *PTEN* CKO mice

(A and B) *In situ* hybridization reveals significantly elevated expression of TRPV1 (A) and MrgprA3 (B) in the DRG neurons of *PTEN* CKO mice relative to that in the controls. TRPV1⁺ and MrgprA3⁺ neurons accounted for 31% and 8%, respectively, of the total DRG neurons in control mice, but these proportions increased to 50% and 12% in *PTEN* CKO mice. Bars represent ±SEM.

(C) The percentage of TRPV1⁺ neurons in GFP⁺ (i.e., Cre) neurons were significantly increased in *PTEN* CKO mice compared with that in control mice (n = 3 for each). Bars represent ±SEM.

(D–F) There were no significant differences in the expression levels of MrgprD (D), NPPB (E), and TRPA1 (F) between the two genotypes (n = 8 for each). Bars represent ±SEM. Student's t test *p < 0.05, **p < 0.01. Scale bar, 25 μm shown in (A) and applies to (B)–(F).

before falling and the duration spent on the rod were observed in the rotarod test (Figures 3F and 3G) between *PTEN* CKO mice and controls. The distance traveled in the open field test was also not altered in *PTEN* CKO mice (Figure 3H), suggesting that *PTEN* deletion does not affect general locomotor activity.

Altered expression of itch-related genes in DRG neurons

To explore the possible molecular mechanism underlying the abnormal itch responses, we examined a battery of genes that are involved in itch sensation in primary sensory neurons (Akiyama and Carstens, 2013; Liu et al., 2009, 2012; Mishra and Hoon, 2013; Shim et al., 2007; Wilson et al., 2011). TRPV1 *in situ* hybridization showed that TRPV1⁺ neurons were present in ~30% of the total population of control mice, whereas this number increased to ~50% in *PTEN* CKO mice (Figure 4A). MrgprA3⁺ neurons occupied a relatively small population (~8%) of DRG neurons in control mice but were present in ~12% of DRG neurons in the CKO mice (Figure 4B). To obtain cellular evidence that the increase in TRPV1⁺ neurons is caused by the deletion of PTEN, above mentioned *Drg11*-CreER: *Rosa26*-stop-YFP (control) and *Rosa26*-stop-YFP: *PTEN* CKO mice were used. Double staining showed that the percentage of TRPV1⁺/GFP⁺ neurons in the total population of GFP⁺ neurons was significantly increased in *PTEN* CKO mice compared with that in controls (Figure 4C). On the other hand, *PTEN* deletion did not affect the percentage of DRG neurons expressing MrgprD, NPPB, or TRPA1 relative to that observed in the controls (Figures 4D–4F).

Ectopic expression of TRPV1 and MrgprA3 in IB4⁺ subpopulation of *PTEN* CKO mice

Our previous study showed that *Drg11*-driven Cre recombinase is expressed in approximately 57% of DRG neurons in all populations, including IB4⁺ neurons (Hu et al., 2012). As PTEN is primarily expressed in the IB4⁺ population, we speculated that PTEN might suppress TRPV1 expression in a cell-autonomous manner, particularly in IB4⁺ neurons. To confirm this hypothesis, we first performed double staining of TRPV1 and IB4. Approximately 16.0% of IB4⁺ DRG neurons were immunopositive for TRPV1 in control mice, whereas ~47.1% of them expressed TRPV1 in *PTEN* CKO mice (Figures 5A–5C). Triple labeling of TRPV1, IB4, and GFP was performed to further confirm that ectopic TRPV1 expression is caused by the deletion of *PTEN* in IB4⁺ neurons. In control mice, few neurons expressed all three markers, although IB4/GFP- (Figure 5D, yellow triangles) and TRPV1/GFP-double-labeled neurons were observed (Figure 5D, light blue triangles). In marked contrast, many neurons in *Rosa26*-stop-YFP: *PTEN* CKO mice were positive for GFP, TRPV1, and IB4 together (Figure 5E, white triangles). Therefore, we demonstrated that TRPV1 is ectopically expressed in *PTEN*-deficient IB4⁺ DRG neurons.

In addition to TRPV1, the number of MrgprA3⁺ neurons was also increased in the DRG neurons of CKO mice. We counted MrgprA3⁺/IB4⁺ neurons in the DRG, and its proportion in the total of IB4⁺ neurons was approximately 11% in controls but increased to 19% in *PTEN* CKO mice (Figure S1A). Thus, MrgprA3 is also ectopically expressed in IB4⁺ DRG neurons of *PTEN* CKO mice.

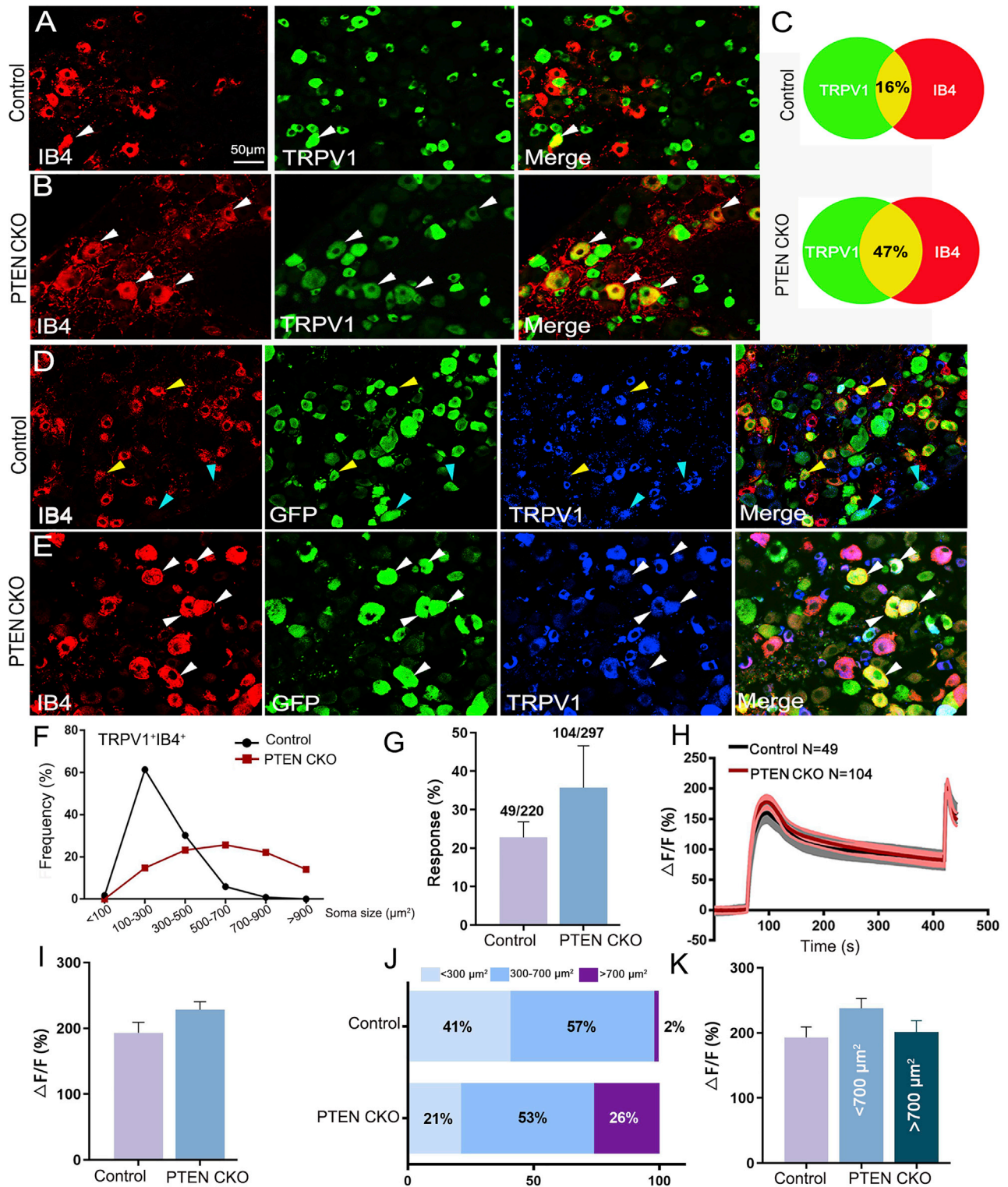**Figure 5. Ectopic expression of TRPV1 in IB4$^+$ neurons of *PTEN* CKO mice**

(A–C) In control mice (A and C), a small proportion (16%) of IB4$^+$ neurons were positive for TRPV1, but nearly half (47%) of them were positive for TRPV1 in *PTEN* CKO mice (B and C). n = 4 for each. White triangles indicate IB4/TRPV1 double-labeled neurons.

(legend continued on next page)

It is well known that deletion of PTEN in neurons leads to a common phenotype of enlarged soma size (Diaz-Ruiz et al., 2009; Li et al., 2003), and as expected, an obvious increase in the soma size of IB4^{+} neurons was observed in *PTEN* CKO mice. The quantification showed that there was an obvious right shift in their proportions along with the increase in soma size in *PTEN* CKO mice (Figure 5F).

Ectopic TPRV1 shows normal capsaicin responsiveness in *PTEN* CKO mice

To further confirm the hypothesis that increased TRPV1 expression in DRG neurons is responsible for abnormal itch responses, it is necessary to examine whether ectopic TRPV1 is functional. To this end, cultured DRG neurons were loaded with the calcium indicator fura-4, whose fluorescence intensity reflects the intracellular calcium concentration as reported in our previous study (Wang et al., 2018). Within 1 min of application of 0.5 μM capsaicin, approximately 22% (49 of 220) of cultured neurons from control mice showed a robust increase in intracellular calcium. This number increased to 35% (104 of 297) in *PTEN* CKO mice (Figure 5G). Calcium signals returned to baseline after a 7-min elution with bath buffer, and the application of KCl caused a second substantial increase in fluorescence intensity, suggesting favorable cellular status. Then, the amplitude of increased fluorescence reflecting the response intensity was quantified, which revealed no significant difference between control and *PTEN* CKO DRG neurons (Figures 5H and 5I). As mentioned before, *PTEN* deletion leads to enlarged soma. We next measured the soma size of the responsive neurons. There was a dramatic increase in the percentage of neurons (∼26%, 27 of 104) with soma areas exceeding 700 μm² in DRG neurons from *PTEN* CKO mice, while only a very small proportion (∼2%, 1 of 49) was found in those from controls (Figure 5J). In addition, capsaicin-responsive neurons with soma areas greater than 700 μm² in *PTEN* CKO analyzed separately to compare the amplitude of increased fluorescence with the other two groups, those with areas less than 700 μm² from *PTEN* CKO and all responsive neurons from controls (Figure 5K). The results showed that there was no significant difference in the amplitude among the three groups. Overall, the ectopically expressed TRPV1 in the DRG neurons of *PTEN* CKO mice exhibits normal responsiveness to its ligand.

The abnormal itch responses were not present in *PTEN: TRPV1* dCKO mice

To investigate whether altered TRPV1 expression in primary sensory neurons is responsible for abnormal itch sensation in *PTEN* CKO mice, we generated *Drg11*-Cre[ER]: *PTEN*[flox/flox]: *TRPV1*[flox/flox] (*PTEN: TRPV1* dCKO) mice. *In situ* hybridization showed that the number of TRPV1^{+} cells was reduced in *PTEN: TRPV1* dCKO mice compared with that of control mice (Figures 6A and 6C), showing successful inactivation of TRPV1 in the DRG neurons of *PTEN: TRPV1* dCKO mice. Critically, the percentage of TRPV1^{+}/IB4^{+} cells in IB4^{+} population of the dCKO mice was reduced with no obvious differences from that of controls (Figures 6B and 6C). Thus, the cellular phenotype of ectopic TRPV1 expression in IB4^{+} DRG neurons was abolished in *PTEN: TRPV1* dCKO mice. We noticed that the phenotype of increased IB4^{+} neuron soma size still existed in the dCKO mice, as shown by the increased proportion of IB4^{+} neurons with a soma size over 700 μm² (Figure 6D). Only ∼2% of the population of neurons in the control mice had the large soma size, whereas this number was approximately 30% in neurons from *PTEN* CKO and *PTEN: TRPV1* dCKO mice (Figure 6E). The increase in the number of MrgprA3^{+} neurons was maintained in the DRG neurons of *PTEN: TRPV1* dCKO mice (Figure S1B).

Next, we assessed itch responses in the dCKO mice using pruritogens including histamine, compound 48/80, chloroquine, and 5-HT and found that the augmented itch response was no longer expressed in *PTEN: TRPV1* dCKO mice and displayed comparable levels relative to control littermates (Figures 6F–6I). It should be noted that no skin lesion or abnormal spontaneous scratching was detected in the dCKO mice (10.0 ± 3.1 in control and 11.0 ± 1.1 in dCKO). Taken together, these results indicate that the ectopic TRPV1 expression is responsible for the elevated itch responses in *PTEN* CKO mice.

Abnormal thermal sensation in *PTEN* CKO and *PTEN: TRPV1* dCKO mice

TRPV1 expressed in DRG neurons is implicated in thermal sensation (Cavanaugh et al., 2009), which may be affected in *PTEN* CKO as a consequence of the increased TRPV1 expression in the DRG neurons. To this end, the tail immersion test and hot plate test were performed. In the tail immersion test, the thermal response was

---

(D and E) Few neurons are triple-labeled with IB4, GFP (i.e., Cre) and TRPV1 in control *Drg11*-Cre[ER]: *Rosa26*-stop-YFP mice (D), whereas many triple-labeled neurons were observed in *PTEN* CKO: *Rosa26*-stop-YFP mice (E). Yellow triangles point to IB4^{+}/GFP^{+} cells, light blue triangles point to GFP[+]/TRPV1^{+} cells, and white triangles indicate IB4^{+}/TRPV1^{+}/GFP^{+} neurons in *PTEN* CKO mice. Scale bars, 50 μm shown in (A) and applies to (B), (D), and (E).

(F) The soma size of IB4^{+}/TRPV1^{+} neurons was increased in the DRG neurons of *PTEN* CKO mice compared with that in control mice. n = 3 for each. A total of 119 and 282 neurons were selected from control and PTEN CKO mice, respectively.

(G) The proportion of DRG neurons with a robust increase in intracellular calcium signals after the application of capsaicin in both genotypes. A total of 220 neurons were recorded with 49 neurons responsive in the control DRG, and 104 responsive neurons in the total of 297 neurons were found in the DRG of *PTEN* CKO. Bars represent ±SEM.

(H) Changes in the fluorescence intensity of DRG neurons during the application of capsaicin.

(I) Quantification of the amplitude of increased fluorescence by capsaicin application revealed no significant differences between controls and *PTEN* CKO mice. Student's t test, n = 49 for control and n = 104 for *PTEN* CKO. Bars represent ±SEM.

(J) Percentages of capsaicin-responsive DRG neurons with different soma size in control and *PTEN* CKO mice. The percentage of neurons with soma area less than 300 μm² was lowered, and correspondingly, that of neurons with soma size exceeding 700 μm² was increased in *PTEN* CKO mice. Soma size is indicated by soma area (μm²).

(K) The amplitudes of increased fluorescence revealed no significant differences among control DRG neurons and *PTEN* CKO DRG neurons with soma size above or below 700 μm². Student's t test. n = 49 for control neurons, n = 77 for DRG neurons with soma size below 700 μm² and n = 27 for DRG neurons with soma sizes above 700 μm² in *PTEN* CKO. Bars represent ±SEM.
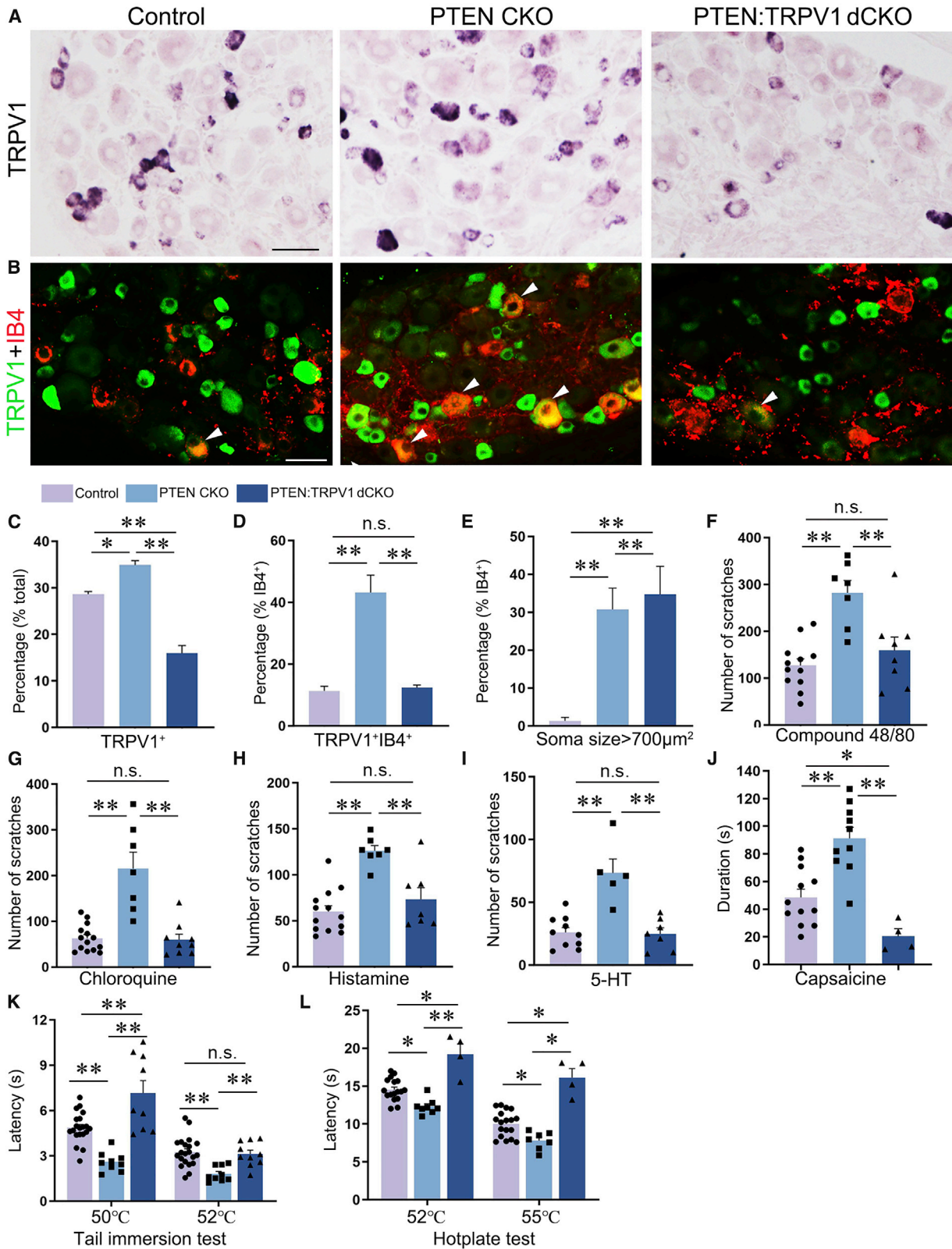
(legend on next page)

scored with the latency of tail flick for water of different temperatures (50°C and 52°C), and it showed that the latency was significantly reduced in CKO mice compared with that of control mice (Figure 6K), showing enhanced thermal sensation in *PTEN* CKO mice. Similar results were obtained in the hot plate test as shown by the reduced latency of the hindpaw flicking, licking, or jumping in the CKO mice relative to controls (Figure 6L). In addition, capsaicin was injected into the plantar of hindpaw, and the CKO mice spent more time in raising, flicking, or licking the hindpaw than control mice (Figure 6J). On the other hand, mechanical nociceptive responses examined with the von Frey filaments displayed a comparable paw withdraw latency in both groups (paw withdraw threshold, 3.05 ± 0.1 in control, 3.1 ± 0.16 in *PTEN* CKO), suggesting unaltered mechanical nociceptive sensation in CKO mice. These behavioral alterations in *PTEN* CKO mice are consistent with the known role of TRPV1 in thermal sensation and chemical nociception.

We next moved to examine how these behaviors were altered in *PTEN*: *TRPV1* dCKO mice. In the tail immersion test, the latency of tail flick at 52°C in the dCKO mice was significantly increased to a level with no difference from control mice, but at 52°C, it was increased to a level higher than that of control mice (Figure 6K). Similar alterations in the thermal sensation were obtained in the hot plate test, as shown by the data that the latency of hindpaw withdraw was increased in the dCKO mice compared with that of *PTEN* CKO mice, but it was longer than that of control mice (Figure 6L). This can be explained by a deletion of endogenous TRPV1 as *Drg11*-driven Cre is expressed in approximately 14.0% of TRPV1+ DRG neurons (Figure 4C), which results in a reduction of TRPV1+ DRG neurons in dCKO mice (Figure 6C). This speculation is also supported by the behavioral data from capsaicin-induced responses in the dCKO mice (Figure 6J). The phenotypes of enhanced thermal sensation and capsaicin-induced nociception in *PTEN* CKO mice are disappeared, but the ability of the two sensory modalities is blunted in *PTEN*: *TRPV1* dCKO mice, which is different from the case of itch-related behaviors mentioned above.

Increased GRP and GRPR expression in the spinal dorsal horn of *PTEN* CKO mice

As TRPV1+ DRG neurons were increased in *PTEN* CKO mice, its central process, as well as those of CGRP, SP, and IB4,

was examined in the dorsal horn. Their distribution patterns in the spinal dorsal horn were not changed, but the density of TRPV1+ terminals was significantly increased, while those of CGRP+, SP+, and IB4+ terminals were not obviously altered in *PTEN* CKO mice relative to that in the controls (Figures S2). Next, we examined the expression of GRP and GRPR, which play essential roles in processing itch sensory information in the spinal cord (Akiyama and Carstens, 2013; Mishra and Hoon, 2013; Sun et al., 2009; Sun and Chen, 2007; Takanami et al., 2021). We found that the numbers of GRP+ neurons and GRPR+ neurons were both increased with an unchanged distribution pattern in *PTEN* CKO mice (Figures 7A–7C). On the other hand, the elevated expression of GRP and GRPR were still detected in *PTEN*: *TRPV1* dCKO mice, with no difference relative to *PTEN* CKO mice (Figures 7A–7C).

To explore the possibility that the increase in GRP and GPRP expression is caused by *PTEN* deletion, we first performed double immunostaining of GFP (i.e., Cre) with PTEN in the dorsal horn of *Drg11*-Cre[ER]: *Rosa26*-stop-YFP mice and found that approximately 85% of GFP+ neurons were labeled with PTEN and that GFP+/PTEN+ neurons constituted about 26% of total PTEN+ neurons (Figure S3A), suggesting PTEN deletion in the dorsal horn of PTEN CKO mice. Next, we examined the colocalization of GFP (i.e., Cre) with GRP and GRPR in the dorsal horn of *Rosa26*-stop-YFP: *PTEN* CKO mice. The results revealed that over half (54%) of GRP+ neurons were labeled with GFP in *Rosa26*-stop-YFP: *PTEN* CKO mice, whereas ~32% were labeled in control mice (Figure 7D). In marked contrast, no colocalization was observed between GRPR and GFP in control or *Rosa26*-stop-YFP: *PTEN* CKO mice (Figure 7E), showing that the increase in GRPR+ neurons is unlikely to be caused by Cre-mediated *PTEN* deletion in the dorsal horn. In addition, we examined the genes expressed in the inhibitory neurons (i.e., SST, DYN, Enkphalin, neuropeptide Y, and Pax2) and excitatory neurons (i.e., Lmx1b, Calbindin, and PKCγ), some of which are implicated in itch processing (Bourane et al., 2015; Duan et al., 2014; Huang et al., 2018; Kardon et al., 2014). The expression and distribution patterns were not obviously different between control and *PTEN* CKO mice (Figures S3B–S3I).

Figure 6. TRPV1 deletion attenuates enhanced itch and thermal sensation in *PTEN* CKO mice

(A and C) *In situ* hybridization showed significantly reduced expression of *TPRV1* in *PTEN*: *TRPV1* dCKO (n = 3) compared with that in control mice (n = 4) and *PTEN* CKO mice (n = 3). Bars represent ±SEM. Scale bars, 50 μm.

(B and D) The percentage of TRPV1+/IB4+ neurons in *PTEN*: *TRPV1* dCKO (n = 3) mice was significantly decreased compared with that in *PTEN* CKO (n = 3) mice, but not significantly different from that in control mice (n = 6). Scale bar, 50 μm. Bars represent ±SEM.

(E) The soma size of IB4+ neurons was still enlarged in *PTEN*: *TRPV1* dCKO mice. The percentage of IB4+ neurons with soma size larger than 700 μm² was approximately 30% in PTEN:TRPV1 dCKO mice (n = 3), similar to that in PTEN CKO mice (n = 3), whereas that population only accounted for ~2% of the IB4+ neurons in control mice (n = 6). Bars represent ±SEM.

(F–I) The number of scratches induced by histamine (H), compound 48/80 (F), chloroquine (G), and 5-HT (I) were dramatically decreased in *PTEN*: *TRPV1* dCKO mice (n = 8) compared with *PTEN* CKO mice (n = 7), but comparable to that in controls (n = 12). Bars represent ±SEM.

(J) The *PTEN* CKO mice (n = 9) spent much more time raising, flicking, or licking the hindpaw after injection of capsaicin than control and meantime, *PTEN*: *TRPV1* dCKO mice (n = 4) spent less time than control mice (n = 8). Bars represent ±SEM.

(K) The thermal sensation was enhanced in *PTEN* CKO mice but blunted in *PTEN*: *TRPV1* dCKO mice shown by data from the tail immersion test. *PTEN* CKO mice (n = 7) displayed a reduced latency relative to that of control mice (n = 12). The latency in *PTEN*: *TRPV1* dCKO mice (n = 9) was increased to a level with no difference from control mice 52°C but to a higher level at 50°C compared with that of control mice. Bars represent ±SEM.

(L) The thermal sensation was enhanced in *PTEN* CKO mice but blunted in *PTEN*: *TRPV1* dCKO mice shown by data from the hot plate test. *PTEN* CKO mice (n = 7) displayed a reduced latency relative to that of control mice (n = 17), but the latency in *PTEN*: *TRPV1* dCKO mice (n = 4) was increased to a level higher than that of control mice. Bars represent ±SEM. One-way ANOVA, *p < 0.05, **p < 0.01, n.s., no significance.
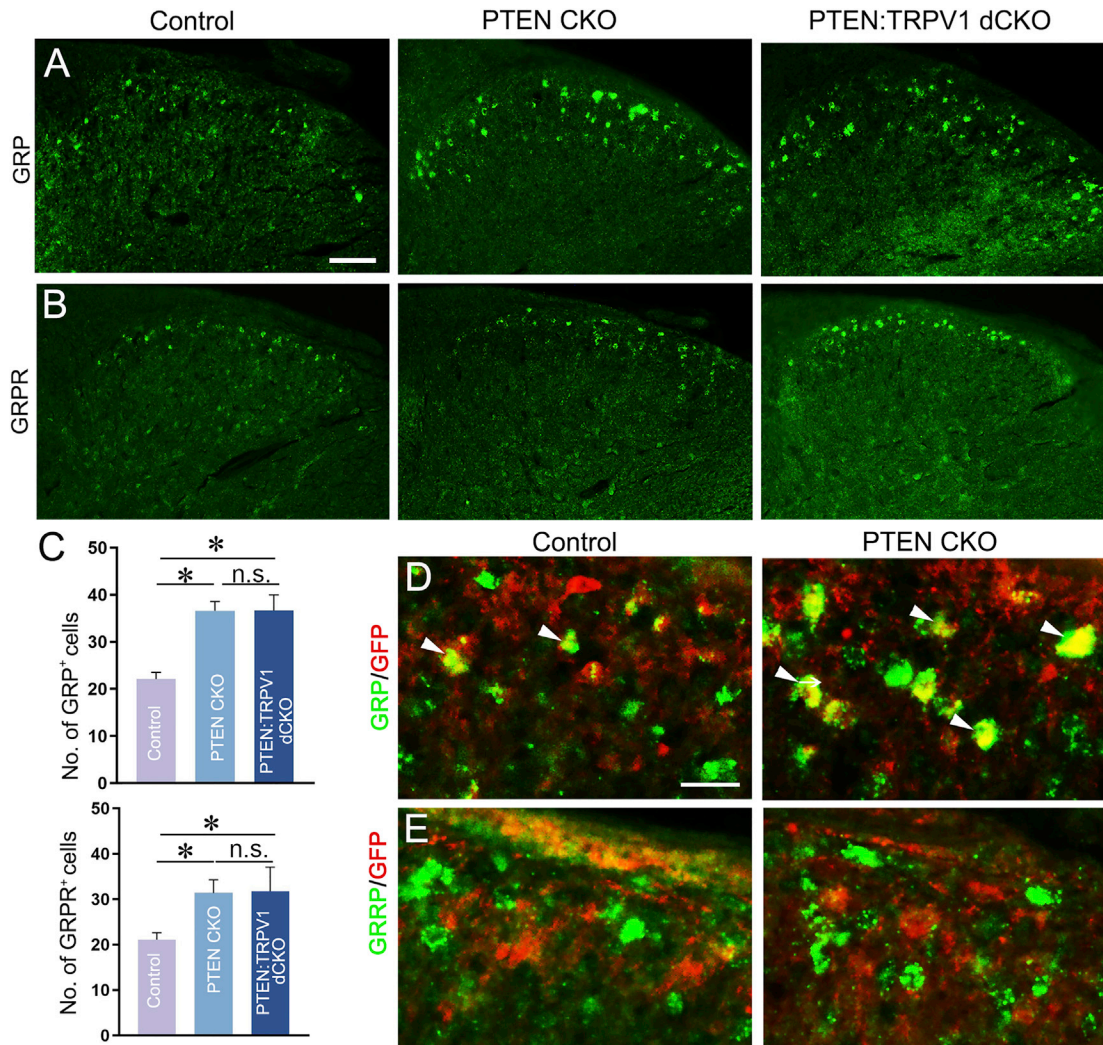
Figure 7. Upregulation of GRP and GRPR in the dorsal horn of *PTEN* CKO mice and *PTEN*: *TRPV1* dCKO mice

(A–C) GRP$^+$ (A and C) neurons and GRPR$^+$ (B and C) neurons were both significantly increased in number in the superficial dorsal horn of *PTEN* CKO mice (n = 7) and *PTEN*:*TRPV1* dCKO mice (n = 5) compared with control mice (n = 5). Bars represent ±SEM. Student's t test, *p < 0.05. Scale bar, 100 μm in (A) and applies in (B).

(D) Approximately 32% (63 of 194) of GRP$^+$ neurons shown by fluorescence *in situ* hybridization were labeled with GFP in control mice, whereas more than half (54.3%, 125 of 230) of GRP$^+$ neurons were positive for GFP in *PTEN* CKO mice. Triangles indicate GFP/GRP-double-labeled neurons in the dorsal horn.

(E) GRPR$^+$ neurons shown by fluorescence *in situ* hybridization were not labeled with GFP in the dorsal horn of control and *Rosa26*-stop-YFP: *PTEN* CKO mice. Scale bar, 100 μm is shown in (A) and applies to (D).

DISCUSSION

In this study, we explored the role of PTEN expressed by DRG neurons in processing itch and thermal information. *PTEN* was inactivated in the DRG neurons of adult mice by inducible Cre activity, thus avoiding the disruption of PTEN-dependent processes during DRG neuron development. *PTEN* CKO mice displayed spontaneous itch and elevated pruritogen-induced itch responses, which were no longer observed in *PTEN*: *TRPV1* dCKO mice. Similarly, thermal sensation and capsaicin-induced responses were also enhanced in *PTEN* CKO mice but were blunted in dCKO mice. At the cellular level, ectopically expressed TRPV1 was observed in the IB4$^+$ population of DRG neurons in *PTEN* CKO mice, and this expression was eliminated

in *PTEN*: *TRPV1* dCKO mice. These results suggest a suppressive role for PTEN in regulating *TRPV1* expression in a population of primary sensory neurons, implicating PTEN in itch and thermal sensation in adult mice.

PTEN expression was inactivated in adult *Drg11*-Cre^{ER} mice, which was confirmed by the loss of *PTEN* in Cre-expressing neurons, the reduction in PTEN expression, and the upregulation of p-Akt levels in the DRG of *PTEN* CKO mice. Consistent with previous studies in rats (Christie et al., 2010), the majority (85%) of PTEN$^+$ neurons were IB4$^+$ DRG neurons, and tamoxifen-induced Cre activity was present in this population (Hu et al., 2012). Thus, the deletion of *PTEN* mainly occurs in IB4$^+$ DRG neurons. Consequently, there was a drastic increase in TRPV1 expression in the IB4$^+$ population (16% in control versus 47% in CKO), as shown

by co-expression of TRPV1 and IB4 by *PTEN*-deficient DRG neurons. However, it should be noted that *PTEN* deletion is not restricted to the IB4^{+} population because *PTEN* is also expressed in approximately 18.7% of IB4-negative DRG neurons, in which inducible Cre activity is also present (Hu et al., 2012). Nevertheless, the changes in gene expression observed in CKO mice are predominately caused by the inactivation of *PTEN* in IB4^{+} DRG neurons.

We explored the molecular mechanism for abnormal itch sensation and observed an increase in TRPV1^{+} and MrgprA3^{+} populations in the DRG neurons, which may underlie the abnormal itch sensation in *PTEN* CKO mice based on the known roles of these two populations in itch transmission (Akiyama and Carstens, 2013; Bautista et al., 2014; Davidson and Giesler, 2010; Han and Dong, 2014; Patel and Dong, 2010). Because the abnormal itch responses were not present in *TRPV1*: *PTEN* dCKO mice, the increase in the TRPV1^{+} DRG population is likely a major contributor to abnormal itch sensation in *PTEN* CKO mice, although MrgprA3 and other unknown mechanisms may also be involved.

At the molecular level, it is likely that PTEN suppresses the expression of itch-related genes in IB4^{+} DRG neurons under physiological conditions. In the absence of PTEN, however, this suppressive mechanism is absent, leading to ectopic expression and, ultimately, abnormal itch sensation. The downstream molecular machinery of PTEN has been well studied (Worby and Dixon, 2014), and further investigation is needed to explore how PTEN regulates itch-related gene expression, especially TRPV1, in DRG neurons. It has been documented that itch represents a common and significant source of morbidity in various cancers (Chiang et al., 2011). Thus, it is of interest to examine whether and how the activity of the PTEN signaling pathway is altered in cancer patients with pruritus, particularly those with *PTEN* mutations.

In addition to the changes in the primary sensory neurons mentioned above, we also observed an increase in GRP[+] and its receptor GRPR[+] populations in the dorsal horn of *PTEN* CKO mice. Double immunostaining showed that a higher proportion of GRP[+]/Cre^{+} spinal neurons was observed in *PTEN* CKO mice than in controls, and the increased GRP[+] population could be attributed to the deletion of *PTEN* in the dorsal horn neurons based on the fact that *Drg11*-driven Cre expression is present in the dorsal horn (Hu et al., 2012). Considering our findings that increased GRP^{+} spinal neurons were still present in *TRPV1:PTEN* dCKO mice with normal itch responses, and a recent report that spinal GRP^{+} neurons are dispensable for itch sensation (Barry et al., 2020), elevated GRP^{+} spinal neurons may not play a major role in abnormal itch sensation in *PTEN* CKO mice. However, unlike GRP^{+} spinal neurons, there was no co-expression of GRPR and Cre in the dorsal horn of *PTEN* CKO or *TRPV1*: *PTEN* dCKO mice. Therefore, it is likely that the increased GRPR expression is secondary to the abnormal itch sensation in the *PTEN* CKO mice. It has been reported that estradiol enhances itch responses in female rats with an increase in GRPR^{+} spinal neurons (Takanami et al., 2021). The contribution of increased GRP[+] and GRPR^{+} spinal neurons to abnormal itch sensation should be explored in future studies, for example, using inducible DRG-specific Cre line.

TRPV1 in DRG neurons is critical for thermal nociception (Caterina et al., 1997, 2000; Davis et al., 2000; Tominaga et al., 1998). The increased TRPV1^{+} population in the DRG of *PTEN* CKO mice could account for the shortened latency in the tail immersion and hot plate tests and augmented capsaicin-induced responses. However, unlike the case of itch-related behaviors that were comparable between control and *PTEN*: *TRPV1* dCKO mice, the thermal sensation and capsaicin-induced nociception were blunted in *TRPV1*: *PTEN* dCKO mice. The difference might be explained by the alterations of other itch molecules (e.g., MrgprA3) that compensate the effect of TPRV1 deletion on itch-related responses in *TRPV1*: *PTEN* dCKO mice.

In summary, our study demonstrated that inactivation of *PTEN* in a subset of DRG neurons leads to abnormal itch and thermal sensation, which can be explained by ectopically expressed TRPV1 in IB4^{+} DRG neurons. Our data not only reveal a novel role of PTEN in the adult brain but also provide a cue for identifying upstream genes controlling itch-related gene expression.

Limitations of the study

The inducible Cre line used in this study has Cre expression in the dorsal horn. On the basis of no colocalization of Cre and GRPR, it is unlikely that the increase of GRPR^{+} neurons are caused by deletion of PTEN in GRPR^{+} neurons and more likely to be a consequence of abnormal itch input carried by PTEN-deficient DRG neurons. However, the colocalization of Cre and GRP in the dorsal horn indicates the possibility that the increase of GRP^{+} neurons is caused by PTEN deletion in the dorsal horn neuron, which consequently contributes to the abnormal itch responses in *PTEN* CKO mice. An inducible and selective DRG Cre line or virus-mediated Cre deliver to adult DRG neurons is needed to address this question. In addition, our study did not provide evidence showing molecular machinery of how PTEN suppresses the expression of TRPV1 or MrgprA3. It is known that itch and nociception are closely associated at the molecular, cellular, and behavioral levels (Ji et al., 2019; Koch et al., 2018; Moore et al., 2018), and additional experiments are needed to explore whether or how other itch- and nociception-related genes are changed, which contribute to the abnormal itch and thermal sensation.

STAR★METHODS

Detailed methods are provided in the online version of this paper and include the following:

- KEY RESOURCES TABLE
- RESOURCE AVAILABILITY
  - Lead contact
  - Materials availability
  - Data and code availability
- EXPERIMENTAL MODEL AND SUBJECT DETAILS
  - Animals
  - Primary DRG neuronal culture
- METHOD DETAILS
  - Immunohistochemistry
  - *In situ* hybridization
  - Western blot

- ○ Behavioral tests
- ○ Ca^{2+} imaging
- ○ Cell counting and soma area measurement
- QUANTIFICATION AND STATISTICAL ANALYSIS

AUTHOR CONTRIBUTIONS

Y.-Q.D. and Q.-X.W. conceived the studies and designed the experiments. L.H., G.-Y.J., and Y.-P.W. carried out the behavioral and immunofluorescence experiments, *in situ* hybridization, and Ca^{2+} imaging. Z.-B.H., B.-Y.Z., J.-L.L., and G.-D.C. assisted with data analysis. L.Z., L.X., Y.L., and B.L. discussed the results and provided technical support. N.-N.S., Y.H., and J.-Y.C. generated and bred the mice. Y.-Q.D., L.H., and G.-Y.J. wrote the manuscript with input from the other authors. All authors discussed and commented on the manuscript.

DECLARATION OF INTERESTS

The authors declare no competing interests.

REFERENCES

Akiyama, T., and Carstens, E. (2013). Neural processing of itch. Neuroscience *250*, 697–714.

Barry, D.M., Liu, X.T., Liu, B., Liu, X.Y., Gao, F., Zeng, X., Liu, J., Yang, Q., Wilhelm, S., Yin, J., et al. (2020). Exploration of sensory and spinal neurons expressing gastrin-releasing peptide in itch and pain related behaviors. Nat. Commun. *11*, 1397.

Bautista, D.M., Wilson, S.R., and Hoon, M.A. (2014). Why we scratch an itch: the molecules, cells and circuits of itch. Nat. Neurosci. *17*, 175–182.

Bourane, S., Duan, B., Koch, S.C., Dalet, A., Britz, O., Garcia-Campmany, L., Kim, E., Cheng, L., Ghosh, A., Ma, Q., et al. (2015). Gate control of mechanical itch by a subpopulation of spinal cord interneurons. Science *350*, 550–554.

Braz, J., Solorzano, C., Wang, X., and Basbaum, A.I. (2014). Transmitting pain and itch messages: a contemporary view of the spinal cord circuits that generate gate control. Neuron *82*, 522–536.

Butler, M.G., Dasouki, M.J., Zhou, X.P., Talebizadeh, Z., Brown, M., Takahashi, T.N., Miles, J.H., Wang, C.H., Stratton, R., Pilarski, R., et al. (2005). Subset of individuals with autism spectrum disorders and extreme macrocephaly associated with germline PTEN tumour suppressor gene mutations. J. Med. Genet. *42*, 318–321.

Caterina, M.J., Leffler, A., Malmberg, A.B., Martin, W.J., Trafton, J., Petersen-Zeitz, K.R., Koltzenburg, M., Basbaum, A.I., and Julius, D. (2000). Impaired nociception and pain sensation in mice lacking the capsaicin receptor. Science *288*, 306–313.

Caterina, M.J., Schumacher, M.A., Tominaga, M., Rosen, T.A., Levine, J.D., and Julius, D. (1997). The capsaicin receptor: a heat-activated ion channel in the pain pathway. Nature *389*, 816–824.

Cavanaugh, D.J., Lee, H., Lo, L., Shields, S.D., Zylka, M.J., Basbaum, A.I., and Anderson, D.J. (2009). Distinct subsets of unmyelinated primary sensory fibers mediate behavioral responses to noxious thermal and mechanical stimuli. Proc. Natl. Acad. Sci. U S A *106*, 9075–9080.

Chaplan, S.R., Bach, F.W., Pogrel, J.W., Chung, J.M., and Yaksh, T.L. (1994). Quantitative assessment of tactile allodynia in the rat paw. J. Neurosci. Methods *53*, 55–63.

Chen, L., Gong, W.K., Yang, C.P., Shao, C.C., Song, N.N., Chen, J.Y., Zhou, L.Q., Zhang, K.S., Li, S., Huang, Z., et al. (2021). Pten is a key intrinsic factor regulating raphe 5-HT neuronal plasticity and depressive behaviors in mice. Transl. Psychiatry *11*, 186.

Chiang, H.C., Huang, V., and Cornelius, L.A. (2011). Cancer and itch. Semin. Cutan. Med. Surg. *30*, 107–112.

Christie, K.J., Webber, C.A., Martinez, J.A., Singh, B., and Zochodne, D.W. (2010). PTEN inhibition to facilitate intrinsic regenerative outgrowth of adult peripheral axons. J. Neurosci. *30*, 9306–9315.

Dai, J.-X., Hu, Z.-L., Shi, M., Guo, C., and Ding, Y.-Q. (2008). Postnatal ontogeny of the transcription factor Lmx1b in the mouse central nervous system. J. Comp. Neurol. *509*, 341–355.

Davidson, S., and Giesler, G.J. (2010). The multiple pathways for itch and their interactions with pain. Trends Neurosci. *33*, 550–558.

Davidson, S., Zhang, X., Khasabov, S.G., Simone, D.A., and Giesler, G.J., Jr. (2009). Relief of itch by scratching: state-dependent inhibition of primate spinothalamic tract neurons. Nat. Neurosci. *12*, 544–546.

Davis, J.B., Gray, J., Gunthorpe, M.J., Hatcher, J.P., Davey, P.T., Overend, P., Harries, M.H., Latcham, J., Clapham, C., Atkinson, K., et al. (2000). Vanilloid receptor-1 is essential for inflammatory thermal hyperalgesia. Nature *405*, 183–187.

Di Cristofano, A., Pesce, B., Cordon-Cardo, C., and Pandolfi, P.P. (1998). Pten is essential for embryonic development and tumour suppression. Nat. Genet. *19*, 348–355.

Diaz-Ruiz, O., Zapata, A., Shan, L., Zhang, Y., Tomac, A.C., Malik, N., de la Cruz, F., and Backman, C.M. (2009). Selective deletion of PTEN in dopamine neurons leads to trophic effects and adaptation of striatal medium spiny projecting neurons. PLoS One *4*, e7027.

Dibble, C.C., and Cantley, L.C. (2015). Regulation of mTORC1 by PI3K signaling. Trends Cell Biol. *25*, 545–555.

Dong, X., Han, S., Zylka, M.J., Simon, M.I., and Anderson, D.J. (2001). A diverse family of GPCRs expressed in specific subsets of nociceptive sensory neurons. Cell *106*, 619–632.

Duan, B., Cheng, L., Bourane, S., Britz, O., Padilla, C., Garcia-Campmany, L., Krashes, M., Knowlton, W., Velasquez, T., Ren, X., et al. (2014). Identification of spinal circuits transmitting and gating mechanical pain. Cell *159*, 1417–1432.

Goffin, A., Hoefsloot, L.H., Bosgoed, E., Swillen, A., and Fryns, J.P. (2001). PTEN mutation in a family with Cowden syndrome and autism. Am. J. Med. Genet. *105*, 521–524.

Gracheva, E.O., Cordero-Morales, J.F., Gonzalez-Carcacia, J.A., Ingolia, N.T., Manno, C., Aranguren, C.I., Weissman, J.S., and Julius, D. (2011). Ganglion-specific splicing of TRPV1 underlies infrared sensation in vampire bats. Nature *476*, 88–91.

Gregorian, C., Nakashima, J., Le Belle, J., Ohab, J., Kim, R., Liu, A., Smith, K.B., Groszer, M., Garcia, A.D., Sofroniew, M.V., et al. (2009). Pten deletion in adult neural stem/progenitor cells enhances constitutive neurogenesis. J. Neurosci. *29*, 1874–1886.

Groszer, M., Erickson, R., Scripture-Adams, D.D., Lesche, R., Trumpp, A., Zack, J.A., Kornblum, H.I., Liu, X., and Wu, H. (2001). Negative regulation of

neural stem/progenitor cell proliferation by the Pten tumor suppressor gene in vivo. Science 294, 2186–2189.

Han, L., and Dong, X. (2014). Itch mechanisms and circuits. Annu. Rev. Biophys. 43, 331–355.

Han, L., Ma, C., Liu, Q., Weng, H.J., Cui, Y., Tang, Z., Kim, Y., Nie, H., Qu, L., Patel, K.N., et al. (2013). A subpopulation of nociceptors specifically linked to itch. Nat. Neurosci. 16, 174–182.

Hu, Z.L., Huang, Y., Tao, X.R., Qi, Z.H., Chen, J.Y., and Ding, Y.Q. (2012). Inducible Prrxl1-CreER(T2) recombination activity in the somatosensory afferent pathway. Genesis 50, 552–560.

Huang, J., Polgar, E., Solinski, H.J., Mishra, S.K., Tseng, P.Y., Iwagaki, N., Boyle, K.A., Dickie, A.C., Kriegbaum, M.C., Wildner, H., et al. (2018). Circuit dissection of the role of somatostatin in itch and pain. Nat. Neurosci. 21, 707–716.

Huang, M., Huang, T., Xiang, Y., Xie, Z., Chen, Y., Yan, R., Xu, J., and Cheng, L. (2008). Ptf1a, Lbx1 and Pax2 coordinate glycinergic and peptidergic transmitter phenotypes in dorsal spinal inhibitory neurons. Dev. Biol. 322, 394–405.

Imamachi, N., Goon, H.P., Lee, H., Anderson, D.J., Simon, M.I., Basbaum, A.I., and Han, S.K. (2009). TRPV1-expressing primary afferents generate behavioral responses to pruritogens via multiple mechanisms. Proc. Natl. Acad. Sci. U S A 106, 11330–11335.

Inagaki, N., Nakamura, N., Nagao, M., Musoh, K., Kawasaki, H., and Nagai, H. (1999). Participation of histamine H1 and H2 receptors in passive cutaneous anaphylaxis-induced scratching behavior in ICR mice. Eur. J. Pharmacol. 367, 361–371.

Ji, R.R., Donnelly, C.R., and Nedergaard, M. (2019). Astrocytes in chronic pain and itch. Nat. Rev. Neurosci. 20, 667–685.

Jiang, G.-Y., Dai, M.-H., Huang, K., Chai, G.-D., Chen, J.-Y., Chen, L., Lang, B., Wang, Q.-X., St Clair, D., McCaig, C., et al. (2015). Neurochemical characterization of pERK-expressing spinal neurons in histamine-induced itch. Sci. Rep. 5, 12787.

Kardon, A.P., Polgar, E., Hachisuka, J., Snyder, L.M., Cameron, D., Savage, S., Cai, X., Karnup, S., Fan, C.R., Hemenway, G.M., et al. (2014). Dynorphin acts as a neuromodulator to inhibit itch in the dorsal horn of the spinal cord. Neuron 82, 573–586.

Kim, D.K., Kim, H.J., Kim, H., Koh, J.Y., Kim, K.M., Noh, M.S., Kim, J.J., and Lee, C.H. (2008). Involvement of serotonin receptors 5-HT1 and 5-HT2 in 12(S)-HPETE-induced scratching in mice. Eur. J. Pharmacol. 579, 390–394.

Koch, S.C., Acton, D., and Goulding, M. (2018). Spinal circuits for touch, pain, and itch. Annu. Rev. Physiol. 80, 189–217.

Koga, K., Chen, T., Li, X.Y., Descalzi, G., Ling, J., Gu, J., and Zhuo, M. (2011). Glutamate acts as a neurotransmitter for gastrin releasing peptide-sensitive and insensitive itch-related synaptic transmission in mammalian spinal cord. Mol. Pain 7, 47.

Kwon, C.H., Luikart, B.W., Powell, C.M., Zhou, J., Matheny, S.A., Zhang, W., Li, Y., Baker, S.J., and Parada, L.F. (2006). Pten regulates neuronal arborization and social interaction in mice. Neuron 50, 377–388.

Lagerström, M.C., Rogoz, K., Abrahamsen, B., Persson, E., Reinius, B., Nordenankar, K., Ölund, C., Smith, C., Mendez, J.A., Chen, Z.F., et al. (2010). VGLUT2-Dependent sensory neurons in the TRPV1 population regulate pain and itch. Neuron 68, 529–542.

Lawson, S.N., and Waddell, P.J. (1991). Soma neurofilament immunoreactivity is related to cell size and fibre conduction velocity in rat primary sensory neurons. J. Physiol. 435, 41–63.

Lesche, R., Groszer, M., Gao, J., Wang, Y., Messing, A., Sun, H., Liu, X., and Wu, H. (2002). Cre/loxP-mediated inactivation of the murine Pten tumor suppressor gene. Genesis 32, 148–149.

Li, J., Yen, C., Liaw, D., Podsypanina, K., Bose, S., Wang, S.I., Puc, J., Miliaresis, C., Rodgers, L., McCombie, R., et al. (1997). PTEN, a putative protein tyrosine phosphatase gene mutated in human brain, breast, and prostate cancer. Science 275, 1943–1947.

Li, L., Liu, F., and Ross, A.H. (2003). PTEN regulation of neural development and CNS stem cells. J. Cell Biochem. 88, 24–28.

Li, T., Wang, G., Hui, V.C.C., Saad, D., de Sousa Valente, J., La Montanara, P., and Nagy, I. (2021). TRPV1 feed-forward sensitisation depends on COX2 up-regulation in primary sensory neurons. Sci. Rep. 11, 3514.

Liu, Q., Sikand, P., Ma, C., Tang, Z., Han, L., Li, Z., Sun, S., LaMotte, R.H., and Dong, X. (2012). Mechanisms of itch evoked by beta-alanine. J. Neurosci. 32, 14532–14537.

Liu, Q., Tang, Z., Surdenikova, L., Kim, S., Patel, K.N., Kim, A., Ru, F., Guan, Y., Weng, H.J., Geng, Y., et al. (2009). Sensory neuron-specific GPCR Mrgprs are itch receptors mediating chloroquine-induced pruritus. Cell 139, 1353–1365.

Liu, Q., Weng, H.J., Patel, K.N., Tang, Z., Bai, H., Steinhoff, M., and Dong, X. (2011). The distinct roles of two GPCRs, MrgprC11 and PAR2, in itch and hyperalgesia. Sci. Signal. 4, ra45.

Liu, T., Xu, Z.Z., Park, C.K., Berta, T., and Ji, R.R. (2010a). Toll-like receptor 7 mediates pruritus. Nat. Neurosci. 13, 1460–1462.

Liu, Y., Abdel Samad, O., Zhang, L., Duan, B., Tong, Q., Lopes, C., Ji, R.R., Lowell, B.B., and Ma, Q. (2010b). VGLUT2-dependent glutamate release from nociceptors is required to sense pain and suppress itch. Neuron 68, 543–556.

McQueen, D.S., Noble, M.A.H., and Bond, S.M. (2007). Endothelin-1 activates ETA receptors to cause reflex scratching in BALB/c mice. Br. J. Pharmacol. 151, 278–284.

Mishra, S.K., and Hoon, M.A. (2013). The cells and circuitry for itch responses in mice. Science 340, 968–971.

Moore, C., Gupta, R., Jordt, S.E., Chen, Y., and Liedtke, W.B. (2018). Regulation of pain and itch by TRP channels. Neurosci. Bull. 34, 120–142.

Mu, D., Deng, J., Liu, K.F., Wu, Z.Y., Shi, Y.F., Guo, W.M., Mao, Q.Q., Liu, X.J., Li, H., and Sun, Y.G. (2017). A central neural circuit for itch sensation. Science 357, 695–699.

Park, K.K., Liu, K., Hu, Y., Smith, P.D., Wang, C., Cai, B., Xu, B., Connolly, L., Kramvis, I., Sahin, M., et al. (2008). Promoting axon regeneration in the adult CNS by modulation of the PTEN/mTOR pathway. Science 322, 963–966.

Patel, K.N., and Dong, X. (2010). An itch to be scratched. Neuron 68, 334–339.

Reddy, V.B., Iuga, A.O., Shimada, S.G., LaMotte, R.H., and Lerner, E.A. (2008). Cowhage-evoked itch is mediated by a novel cysteine protease: a ligand of protease-activated receptors. J. Neurosci. 28, 4331–4335.

Roberson, D.P., Gudes, S., Sprague, J.M., Patoski, H.A.W., Robson, V.K., Blasl, F., Duan, B., Oh, S.B., Bean, B.P., Ma, Q., et al. (2013). Activity-dependent silencing reveals functionally distinct itch-generating sensory neurons. Nat. Neurosci. 16, 910–918.

Ross, S.E. (2011). Pain and itch: insights into the neural circuits of aversive somatosensation in health and disease. Curr. Opin. Neurobiol. 21, 880–887.

Ross, S.E., Mardinly, A.R., McCord, A.E., Zurawski, J., Cohen, S., Jung, C., Hu, L., Mok, S.I., Shah, A., Savner, E.M., et al. (2010). Loss of inhibitory interneurons in the dorsal spinal cord and elevated itch in Bhlhb5 mutant mice. Neuron 65, 886–898.

Rossbach, K., Wendorff, S., Sander, K., Stark, H., Gutzmer, R., Werfel, T., Kietzmann, M., and Bäumer, W. (2009). Histamine H4 receptor antagonism reduces hapten-induced scratching behaviour but not inflammation. Exp. Dermatol. 18, 57–63.

Shi, M., Hu, Z.-L., Zheng, M.-H., Song, N.-N., Huang, Y., Zhao, G., Han, H., and Ding, Y.-Q. (2012). Notch–Rbpj signaling is required for the development of noradrenergic neurons in the mouse locus coeruleus. J. Cell Sci. 125, 4320–4332.

Shim, W.S., Tak, M.H., Lee, M.H., Kim, M., Kim, M., Koo, J.Y., Lee, C.H., Kim, M., and Oh, U. (2007). TRPV1 mediates histamine-induced itching via the activation of phospholipase A2 and 12-lipoxygenase. J. Neurosci. 27, 2331–2337.

Silverman, J.D., and Kruger, L. (1988). Lectin and neuropeptide labeling of separate populations of dorsal root ganglion neurons and associated "nociceptor" thin axons in rat testis and cornea whole-mount preparations. Somatosens. Res. 5, 259–267.

Steck, P.A., Pershouse, M.A., Jasser, S.A., Yung, W.K.A., Lin, H., Ligon, A.H., Langford, L.A., Baumgard, M.L., Hattier, T., Davis, T., et al. (1997).

Identification of a candidate tumour suppressor gene, MMAC1, at chromosome 10q23.3 that is mutated in multiple advanced cancers. Nat. Genet. *15*, 356–362.

Steinhoff, M., Neisius, U., Ikoma, A., Fartasch, M., Heyer, G., Skov, P.S., Luger, T.A., and Schmelz, M. (2003). Proteinase-activated receptor-2 mediates itch: a novel pathway for pruritus in human skin. J. Neurosci. *23*, 6176–6180.

Steinhoff, M., Vergnolle, N., Young, S.H., Tognetto, M., Amadesi, S., Ennes, H.S., Trevisani, M., Hollenberg, M.D., Wallace, J.L., Caughey, G.H., et al. (2000). Agonists of proteinase-activated receptor 2 induce inflammation by a neurogenic mechanism. Nat. Med. *6*, 151–158.

Sun, S., Xu, Q., Guo, C., Guan, Y., Liu, Q., and Dong, X. (2017). Leaky gate model: intensity-dependent coding of pain and itch in the spinal cord. Neuron *93*, 840–853.e5.

Sun, Y.-G., Zhao, Z.-Q., Meng, X.-L., Yin, J., Liu, X.-Y., and Chen, Z.-F. (2009). Cellular basis of itch sensation. Science *325*, 1531–1534.

Sun, Y.G., and Chen, Z.F. (2007). A gastrin-releasing peptide receptor mediates the itch sensation in the spinal cord. Nature *448*, 700–703.

Suzuki, A., De La Pompa, J.L., Stambolic, V., Elia, A.J., Sasaki, T., Del Barco Barrantes, I., Ho, A., Wakeham, A., Itie, A., Khoo, W., et al. (1998). High cancer susceptibility and embryonic lethality associated with mutation of the PTEN tumor suppressor gene in mice. Curr. Biol. *8*, 1169–1178.

Takanami, K., Uta, D., Matsuda, K.I., Kawata, M., Carstens, E., Sakamoto, T., and Sakamoto, H. (2021). Estrogens influence female itch sensitivity via the spinal gastrin-releasing peptide receptor neurons. Proc. Natl. Acad. Sci. U S A *118*, e2103536118.

Than, J.Y., Li, L., Hasan, R., and Zhang, X. (2013). Excitation and modulation of TRPA1, TRPV1, and TRPM8 channel-expressing sensory neurons by the pruritogen chloroquine. J. Biol. Chem. *288*, 12818–12827.

Tominaga, M., Caterina, M.J., Malmberg, A.B., Rosen, T.A., Gilbert, H., Skinner, K., Raumann, B.E., Basbaum, A.I., and Julius, D. (1998). The cloned capsaicin receptor integrates multiple pain-producing stimuli. Neuron *21*, 531–543.

Wang, X.Q., Zhang, L., Xia, Z.Y., Chen, J.Y., Fang, Y., and Ding, Y.Q. (2021). PTEN in prefrontal cortex is essential in regulating depression-like behaviors in mice. Transl. Psychiatry *11*, 185.

Wang, Y., Gao, Y., Tian, Q., Deng, Q., Wang, Y., Zhou, T., Liu, Q., Mei, K., Wang, Y., Liu, H., et al. (2018). TRPV1 SUMOylation regulates nociceptive signaling in models of inflammatory pain. Nat. Commun. *9*, 1529.

Wilson, S.R., Gerhold, K.A., Bifolck-Fisher, A., Liu, Q., Patel, K.N., Dong, X., and Bautista, D.M. (2011). TRPA1 is required for histamine-independent, Mas-related G protein-coupled receptor-mediated itch. Nat. Neurosci. *14*, 595–602.

Worby, C.A., and Dixon, J.E. (2014). PTEN. Annu. Rev. Biochem. *83*, 641–669.

Yamaguchi, T., Nagasawa, T., Satoh, M., and Kuraishi, Y. (1999). Itch-associated response induced by intradermal serotonin through 5-HT2 receptors in mice. Neurosci. Res. *35*, 77–83.

Zhang, L., Jiang, G.-Y., Song, N.-J., Huang, Y., Chen, J.-Y., Wang, Q.-X., and Ding, Y.-Q. (2014). Extracellular signal-regulated kinase (ERK) activation is required for itch sensation in the spinal cord. Mol. Brain *7*, 25.

Zhou, Y., Suzuki, Y., Uchida, K., and Tominaga, M. (2013). Identification of a splice variant of mouse TRPA1 that regulates TRPA1 activity. Nat. Commun. *4*, 2399.

Zori, R.T., Marsh, D.J., Graham, G.E., Marliss, E.B., and Eng, C. (1998). Germline PTEN mutation in a family with Cowden syndrome and Bannayan-Riley-Ruvalcaba syndrome. Am. J. Med. Genet. *80*, 399–402.

STAR★METHODS

KEY RESOURCES TABLE

REAGENT or RESOURCE	SOURCE	IDENTIFIER
Antibodies		
Goat anti-TRPV1	Santa Cruz	Cat# sc-12498;RRID:AB_2241046
Mouse anti-PTEN	Cell Signaling	Cat# 9556; RRID:AB_331153
Goat anti-GFP	Novus Biologicals	Cat# NB100-1770; RRID:AB_10128178
Goat anti -CGRP	Abcam	Cat# ab36001; RRID:AB_725807
Guinea pig anti-Substance P	Abcam	Cat# ab106291; RRID:AB_10864733
Anti-IB4	Sigma-Aldrich	Cat# L2140; RRID:AB_2313663
Rabbit anti-TRPA1	Abcam	Cat# ab68847; RRID:AB_2209954
Mouse anti-NF200	Abcam	Cat# ab7795; RRID:AB_306084
Rabbit anti -Pax2	ThermoFisher	Cat# 71-6000; RRID:AB_2533990
Rabbit anti-Lmx1b	Dai et al., 2008	N/A
Rabbit anti-Calbinidn	Sigma-Aldrich	Cat# HPA023099; RRID:AB_1845859
Donkey anti-rabbit, IgG H&L (HRP)	Abcam	Cat#ab6802; RRID: AB_955445
Rabbit anti-phospho-Akt-Ser473	Cell Signaling	Cat# 4060; RRID:AB_2315049
Anti-PKC gamma antibody	Santa Cruz	Cat# sc-166385; RRID:AB_2018059
Alexa488-conjugated, donkey-anti-rabbit	ThermoFisher	Cat# A-21206; RRID:AB_2535792
Biotin-conjugated, horse-anti-rabbit	Vector Laboratories	Cat# BA-1000; RRID:AB_2313606
Biotin-conjugated, horse-anti-goat	Vector Laboratories	Cat# BA-5000; RRID:AB_2336126
Biotin-conjugated, horse-anti-mouse	Vector Laboratories	Cat# BA-2000; RRID:AB_2313581
Biotin-conjugated, horse-anti- Guinea pig	Vector Laboratories	Cat# BA-7000; RRID:AB_2336132
Alexa488-conjugated, donkey-anti-goat	ThermoFisher	Cat# A32814; RRID:AB_2762838
Alexa488-conjugated, donkey-anti-mouse	ThermoFisher	Cat# A32766; RRID:AB_2762823
Cyanine5, Goat anti-Rabbit	ThermoFisher	Cat# A10523; RRID:AB_2534032
Cy™3-conjugated Streptavidin	Jackson Immunoresearch	Cat# 016-160-084; RRID:AB_2337244
Anti-Digoxigenin-AP	Sigma-Aldrich	Cat# 11093274910; RRID:AB_2734716
Sheep Anti-Digoxigenin-POD	Roche	Cat# 11207733910; RRID:AB_514500
Rabbit anti-GAPDH	Santa Cruz	Cat# sc-32233; RRID:AB_627679
Chemicals, peptides, and recombinant proteins		
Histamine	Sigma-Aldrich	Cat# H7125
Compound48/80	Sigma-Aldrich	Cat# C2313
Chloroquine	Sigma-Aldrich	Cat# C6628
5-HT	Sigma-Aldrich	Cat# H7752
PAR2 agonist	Sigma-Aldrich	Cat# S9317
Capsaicin	Sigma-Aldrich	Cat# M2028
Collagenase-II	Sigma-Aldrich	Cat# C9891
Trypsin	Gibco	Cat# T8003
HBSS buffer	Gibco	Cat# 14170161
DMEM/F-12	Gibco	Cat# 11320033
Fluo-4-AM	ThermoFisher	Cat# F14201
Hoechst	ThermoFisher	Cat# H21486
DNase	Gibco	Cat# DN25
OCT	Tissue-Tek	Cat# 4583
Tween-20	Sangon	Cat# A100777
Tamoxifen	Sigma-Aldrich	Cat# T5648
3,3-diaminobenzidine	Sigma-Aldrich	Cat# 8001

Continued

REAGENT or RESOURCE	SOURCE	IDENTIFIER
Triton-100 X	Sangon	Cat# A110694
T7 polymerase	Promega	Cat# P207C
SP6 polymerase	Promega	Cat# P108B
TSA Plus Biotin Kit	Perkin Elmer	Cat# 2087344
VECTASTAIN ABC Kit	Vector Laboratories	Cat# PK4000
Western HRP Substrate	Millipore	Cat# WBLUR0100
Experimental models: Organisms/strains		
Mouse: PTEN$^{flox/flox}$ mice	Lesche et al., 2002	N/A
Mouse: TRPV1$^{flox/flox}$ mice	Nanjing Biomedical Research Institute	N/A
Mouse: Drg11-Cre^{ER} mice	Hu et al., 2012	N/A
Recombinant DNA		
PGEM-TRPV1	This paper	N/A
PGEM-MrgprA3	This paper	N/A
PGEM- MrgprD	This paper	N/A
PGEM-NPPB	This paper	N/A
PGEM-NPY	This paper	N/A
PGEM-SST	This paper	N/A
PGEM-ENK	This paper	N/A
PGEM-DYN	This paper	N/A
Software and algorithms		
ImageJ	NIH	https://imagej.net/Welcome
GraphPad Prism	GraphPad Software	https://www.graphpad.com/scientificsoftware/prism/
EthoVision XT Noldus	Noldus	https://www.noldus.com/ethovision-xt
Adobe Photoshop CS6	Adobe	https://www.adobe.com/

RESOURCE AVAILABILITY

Lead contact
Further information and requests for resources and reagents should be directed to and will be fulfilled by the Lead contact, Yu-Qiang Ding (dingyuqiang@vip.163.com).

Materials availability
All unique/stable materials will be made available upon reasonable request from the Lead contact without restriction.

Data and code availability
- All data reported in this paper will be shared by the Lead contact upon request.
- This paper does not report original code.
- Any additional information required to reanalyze the data reported in this work paper is available from the Lead contact upon request.

EXPERIMENTAL MODEL AND SUBJECT DETAILS

Animals
PTEN$^{flox/flox}$ mice and Drg11-Cre^{ER} mice were used to acquire PTEN CKO (Drg11-Cre^{ER}: PTE N$^{flox/flox}$). Then, TRPV1$^{flox/flox}$ mice (loxP-flanked exon 10, Nanjing Biomedical Research Institute, Nanjing, China) were crossed with Drg11-Cre^{ER}: PTEN$^{flox/+}$ to obtain Drg11-Cre^{ER}; PTEN$^{flox/+}$; TRPV1$^{flox/+}$. After another round crossing, PTEN: TRPV1 dCKO (Drg11-Cre^{ER}; PTEN$^{flox/flox}$; TRPV1$^{flox/flox}$) were generated by mating Drg11-Cre^{ER}; PTEN $^{flox/+}$; TRPV1$^{flox/+}$ with PTEN$^{flox/+}$; TRPV1$^{flox/+}$. The genotype of CKO mice and dCKO was determined by performing three parallel PCRs using three pairs of primers (PTEN flox: F: ACTCAAGGCAGGGATGAGC; R: GCTGTGGTGGGTTATGGTCTTC; TRPV1 flox: F: AACCCATCCTGCACAGAGGCTT; R: TGAGCCTGCCCTTTGGAACT; Cre: F: ATTTGCCTGCATTACCGGTCG; R: CAGCATTGCTGTCACTTGGTC). PCR was carried out using standard techniques. Two-month-old

PTEN CKO, *PTEN*: *TRPV1* dCKO and control mice were subjected to five intragastric administrations (10 μL/g body weight) of 20 mg/mL tamoxifen dissolved in corn oil in a 2-week paradigm (days 1, 8, 10, 12 and 14). Tamoxifen-treated mice were then raised for another 3–4 weeks for behavior tests. Mice were housed under a 12 h/12 h dark/light cycle with ad libitum access to food and water in the animal facility. The mouse strains used in this study were generated and maintained on the C57BL/6J background, and sex was not controlled in behavioral experiments. All animal experiments were reviewed and approved by the Animal Research Committee of Tongji University School of Medicine and Fudan University, Shanghai, China.

Primary DRG neuronal culture
The lumbar DRGs were quickly isolated and cleaned of adhering connective tissue. Following incubation in digestion solution (1.0 mg/mL collagenase-II, 0.4 mg/mL DNase and 0.1 mg/mL trypsin, dissolved in HBSS buffer) for 30 min at 37°C, the DRG tissue was dispersed in DMEM/F12 containing 10% fetal bovine serum by trituration with glass pipettes. The cell suspension was then transferred onto poly-D-lysine-coated coverslips and incubated at 37°C for 24 hours.

METHOD DETAILS

Immunohistochemistry
Mice were anesthetized with pentobarbital and perfused with 0.1 M PBS followed by 4% paraformaldehyde (PFA). DRGs were dissected, post-fixed in 4% PFA at 4°C overnight, and cryoprotected in 30% sucrose at 4°C for two days. Frozen DRG tissues were cut into 12 μm sections. All sections were incubated in blocking serum containing 0.5% Triton X-100 for 1 h at room temperature, followed by incubating with primary antibodies at 4°C for 12 hours. After primary antibodies incubation, all sections were rinsed with PBS three times and stained with secondary antibodies (Alexa488-conjugated or Biotin-conjugated) at room temperature for 3 hours. For biotin-conjugated secondary antibodies, the sections needed to incubate with cy3-conjugated streptavidin for 1 hour at room temperature. Then, all sections were mounted with 75% glycerol. Images were acquired on an Eclipse fluorescence microscope (Nikon, Tokyo, Japan).

In situ hybridization
DNA fragments of *TRPV1* (Gracheva et al., 2011), *MrgprD* (Dong et al., 2001), *MrgprA3* (Han et al., 2013), *NPPB* (Mishra and Hoon, 2013), *GRP*, *GRPR* (Sun et al., 2009), *DYN*, *ENK*, *NPY* and *SST* (Huang et al., 2008) were cloned into PGEM-T vector and antisense RNA probes were made using T7 or SP6 polymerase. Then, *in situ* hybridization were performed in the DRG sections of *PTEN* CKO and control mice as described in our previous studies (Dai et al., 2008; Shi et al., 2012).

In combination of *in situ* hybridization and IB4 staining, 2 μg/mL protease K was utilized to digest cell membrane protein instead of 10 μg/mL in conventional procedure. After the completion of TRPV1 and MrgprA3 *in situ* hybridization, IB4-biotin (Sigma, L2140) was added and incubated at 4°C overnight. Following the incubation with a mixture of liquid A and B in a 1:200 of dilution from avidin/biotin complex reagent (Vector Laboratories, PK4000) at room temperature for 1 hour, the sections were ready to develop the signal using 3,3-diaminobenzidine (D8001, Sigma Aldrich). Then the slides were washed twice and mounted with coverslips using 75% glycerol.

For fluorescence *in situ* hybridization of GRPR and GRP, similar procedures were conducted in the incubation of antisense probes and consecutive washings but anti-digoxigenin-AP (11093274910, Sigma, 1:2000) used in conventional procedure was replaced with anti-digoxigenin-POD (11207733910, Roche, 1:100). Meanwhile, in the final step, the TSA-FITC in the tyramide signal amplification system (TSA Plus Biotin Kit, PerkinElmer, 2087344) was employed to reveal the signal of GRPR and GRP mRNA.

Western blot
Total protein of DRG and spinal cord were prepared and subjected to western blot as mentioned in our previous study (Zhang et al., 2014). Membranes were incubated overnight at 4°C with primary antibody followed by incubation with HRP-conjugated secondary antibody for 2 hours at room temperature. Signals were developed using the western HRP substrate (WBLUR0500, Millipore).

Behavioral tests
Itch-related behavioral tests
For acute itch sensation assessment, the nape regions of *PTEN* CKO, *TRPV1*: *PTEN* dCKO and control mice were carefully shaved 1 day prior to tests. Intradermal injections of 50 μL PBS-dissolved pruritogens were administered as follows: histamine (10 μg/μL; Sigma, H7125), compound 48/80 (2 μg/μL; Sigma, C2313), chloroquine (4 μg/μL; Sigma, C6628), 5-HT (0.4 μg/μL; Sigma, H7752) and the PAR2 agonist SLIGRL-NH2 (2 μg/μL; Sigma, S9317) (Yamaguchi et al., 1999; Zhang et al., 2014). Scratching behavior was quantified by counting the number of scratches with hind limbs toward the shaved skin within 30 min after administration of pruritogens by a trained observer who was blind to the experimental design. This principle was applied in all behavioral tests.
Capsaicin-induced nociception
The plantar hindpaw was injected with 25 μL PBS-dissolved capsaicin (0.25 μg/μL, Sigma, M2028) and the duration of hindpaw raising, flicking and/or licking in subsequent 3 min was recorded.

Tail immersion test

The tail was placed in a water bath at 50°C and 52°C at 1 cm from the tip. The latency of reflective withdrawal of the tail from the water was recorded. The latency for every temperature was measured at least four times per animal, and tail immersion was limited to 30 s to avoid tissue damage.

Hot plate test

Mice were placed on a hot plate and the latency to hindpaw flicking, licking or jumping was recorded. The hot plate test was conducted at two temperatures (52°C and 55°C). The latency for every temperature was measured at least five times per animal.

Von frey

Basal mechano-nociceptive response was evaluated by applying a series of von frey filaments onto center of the hindpaws as reported previously (Chaplan et al., 1994). Before testing, mice were acclimated for 2 hours in individual chambers. The withdrawal threshold for von frey test was determined as the smallest filament at which at least five positive responses were evoked in ten trials with a 10 s interval.

Rota-rod

Mice were placed on the rotating rod with an accelerating velocity starting from 3.5 rpm/s to 40 rpm/s at 0.2 rpm/s within 5 min. The latency to fall and the falling velocity were recorded.

Open field

PTEN CKO and control mice were placed into the center of the open chamber (42 cm × 42 cm x 42 cm) and allowed for free movement for 30 min. The total distance traveled was analyzed as an indicator of locomotor activity.

Ca^{2+} imaging

The adherent DRG neurons were loaded with the Ca^{2+} indicator Fluo-4-AM (2 μg, diluted in 2 mL bath solution containing 140 mM NaCl, 5 mM KCl, 2 mM $CaCl_2$, 2 mM $MgCl2 \cdot 6H_2O$, 10 mM HEPES and 10 mM glucose with 0.02% Pluronic F-127) at 37°C for 30 min. After dye loading, the coverslip was placed into the recording chamber. Cells were observed under an inverted microscope (Leica BMI4000B, Wetzlar, Germany) and imaged by a CCD camera (Leica DF350, Wetzlar, Germany). Capsaicin (Sigma, 0.5 μM) (Li et al., 2021; Than et al., 2013; Zhou et al., 2013) was perfused by gravity via a microperfusion apparatus for 1 min, and then the neurons were washed with bath solution for 7 min before 3 M KCl was applied to test the cell response. The fluorescence intensity of individual neurons within the region of interest was circled, recorded and analyzed by Leica Advanced Fluorescence Application software (AF 6000; Wetzlar, Germany). The amplitude of increased fluorescence was calculated by subtracting the average baseline from the maximum intensity, dividing the result to the average baseline and multiplying by 100. A positive response was obtained when the fluorescence amplitude increases by capsaicin more than 10%. Only KCl-responsive cells were considered to be excitable cells and the number used as denominator for calculating the proportion of DRG neurons responsive to capsaicin. In addition, the soma size of recorded neurons was also measured using Adobe Photoshop CS6 as mentioned below. The experimenter was blind to the group identity of the tested mice.

Cell counting and soma area measurement

For DRG cell counting, 4–5 sections of lumbar DRGs were randomly selected from each mouse, and 3–6 mice were included for each comparison. Positive DRG neurons with nucleus in sections were included. To measure soma size, $TRPV1^+/IB4^+$ neurons were stringently circled using Adobe Photoshop CS6, and the total pixels of the selected area (the cell soma area) were recorded and subsequently transformed into absolute areas according to the scale bar. For quantification of $TRPV1^+$, SP^+, $CGRP^+$ and $IB4^+$ terminals, the lumbar segments (4th and 5th) were cut into 5 sets of serial sections, and one of them was subjected to the individual staining and quantification.

QUANTIFICATION AND STATISTICAL ANALYSIS

Statistical tests were analyzed with GraphPad Prism (GraphPad Software) and all data are presented as the mean ± SEM. One-way ANOVA was used to analyze the amplitude of increased fluorescence among the three groups and compare the scratching number among control, PTEN CKO and PTEN: TRPV1 dCKO mice. Post-hoc comparisons were made using the Bonferroni test. In the other experiments, differences between control and PTEN CKO mice were measured using Student's t-test. A p value below 0.05 was considered to represent a significant difference.